Combinatorial Treatment of Glioblastoma with Temozolomide (TMZ) Plus 5-Ethynyl-2'-deoxyuridine (EdU)

Humeyra Kaanoglu[1,*], Yasemin K. Akyel[1,*], Adebimpe Adefolaju[2], Alain Valdivia[2], Dominique Higgins[3], Caroline Mosely[4], Corey J. Haswell[4], William C. Zamboni[4], Shawn D. Hingtgen[2], Andrew B. Satterlee[2, 5], and Aziz Sancar[1, 6]

[1]Department of Biochemistry and Biophysics, University of North Carolina School of Medicine, Chapel Hill, North Carolina

[2]Division of Pharmacoengineering and Molecular Pharmaceutics, Eshelman School of Pharmacy University of North Carolina, Chapel Hill, North Carolina

[3]Department of Neurosurgery, University of North Carolina, Chapel Hill, North Carolina

[4]UNC Advanced Translational Pharmacology and Analytical Chemistry Lab, UNC Eshelman School of Pharmacy, University of North Carolina at Chapel Hill, North Carolina

[5]Eshelman Innovation, University of North Carolina, Chapel Hill, North Carolina

[6]**Correspondence:** aziz_sancar@med.unc.edu

[*]Equal contribution

Conflict of Interest Disclosure Statement: Aziz Sancar, Humeyra Kaanoglu and Yasemin Akyel filed a patent application with title "METHODS OF TREATING CANCER OF CENTRAL NERVOUS SYSTEM COMPRISING 5-ETHYNYL-2'-DEOXYURIDINE AND TEMOZOLOMIDE" and U.S. Provisional Application No. 6/893,131 on October 3, 2025.

ABSTRACT

Glioblastoma (GBM) is the most aggressive malignant primary brain tumor in adults, with incidence peaking in later life. It is commonly treated with surgery followed by administration of ionizing radiation and the DNA alkylating agent temozolomide (TMZ). Even though this regimen confers some progression-free survival, there is essentially no cure with the median survival with the standard of care being about 12 months. Currently, several alternative approaches are being developed to improve upon this outcome. We have already shown EdU alone effectively treats GBM, and we now study efficacy of TMZ+EdU combination therapy. TMZ+EdU significantly improves antitumor efficacy compared to either single-agent therapy against GBM cell lines *in vitro*, against 3 different orthotopic GBM xenograft models, and against passage-zero patient GBM tumor tissues engrafted within an organotypic brain slice culture (OBSC)-based platform. Together, these data suggest that EdU could be effective alongside standard of care TMZ in patients with GBM.

STATEMENT OF SIGNIFICANCE (50-WORD)

By simultaneously engaging distinct DNA repair pathways, combination of TMZ and EdU produced unprecedented survival benefits and synergistic effects in preclinical GBM models, offering a promising new avenue in the treatment of GBM.

INTRODUCTION

Despite the application of multidisciplinary treatment approaches combining surgical, radiotherapeutic, and pharmacologic interventions, glioblastoma (GBM) remains one of the most treatment-resistant human cancers, with progression and recurrence as defining features (1–4). At the molecular level, GBM arises through a constellation of genetic alterations, including loss of heterozygosity on chromosome 10q, EGFR amplification, p16INK4a deletion, PTEN mutation, and, at later stages, TP53 and IDH1 mutations (5,6). Currently, the standard of care for GBM consists of surgery followed by ionizing radiation and temozolomide (TMZ) drug therapy (7–9)., During TMZ treatment, eventually MGMT (methylguanine methyl transferase) promoter hypermethylation causes silencing of MGMT which plays an essential role in TMZ-initiated death of malignant tumor cells. However, after an initial positive response to multimodal therapy, ~80% of GBM patients experience recurrence at or near the original tumor site (10–13), often accompanied by new genetic alterations acquired under treatment pressure (14,15). At this stage, therapeutic options are limited, and even with standard of care, median survival remains around 12 months (4,13,16). Recently, a number of new drugs/intervention methods have been developed to improve the management of GBM (17). Among these, 5-ethynyl-2-deoxyuridine (EdU), conceptually, appears to be unique in terms of being immune to resistance development due to its high similarity to thymidine (see **Fig. 1** for the chemical structures of TMZ and EdU).

EdU is commonly used to study DNA replication via "click chemistry" (18–21). During our attempt to employ EdU to analyze nucleotide excision repair patch size in human cell lines, we discovered that EdU incorporated into the human genome is recognized as “damage” and removed from the genome by the classic human dual incision mechanism in the form of 26-27 nt-long oligomers, leading to a futile cycle of incorporation into DNA and its removal (22). This realization, combined with previous reports on toxicity of EdU in tissue culture as well as its established property of crossing the blood brain barrier led to the notion that EdU might be effective against brain cancer (23,24). In our previous study, we showed that EdU is effective against GBM cell lines *in vitro*, orthotopic *in vivo* mouse models of GBM established with intracranial engrafts of mouse glioma and human GBM cells, and living, passage-zero patient GBM tissues tested *ex vivo* on an organotypic brain slice culture (OBSC)-based platform (25). Here, building on these proof-of-concept studies, we sought to investigate the therapeutic potential of combining TMZ with EdU for GBM, reasoning that their distinct mechanisms of action and the conceptual improbability of

resistance to EdU—given its close structural similarity to thymidine—might reduce recurrence rates and even enable durable remission in a subset of patients. To this end, in this study, we tested the synergistic effect of TMZ+EdU in three different GBM cell lines *in vitro*, in *in vivo* orthotopic mouse models of GBM established with these three GBM cell lines, and in living, passage-zero GBM patient tissues seeded on OBSCs. Our results show the combination of TMZ and EdU as a new and promising therapeutic avenue, yielding synergistic effects in GBM and having the potential to ultimately improve the poor prognosis faced by patients with this disease.

RESULTS

Targeted localization and pharmacokinetic features of EdU *in vivo*

In our previous study, we showed the targeted localization of EdU into the human GBM cell lines seeded on OBSCs (25). In this study, we started out by testing the targeted localization of EdU into tumor cells *in vivo*. To this end, we established orthotopic GBM tumors in female athymic nude mice by inoculating FLuc expressing U87 human GBM cells into their brain parenchyma. Since U87 tumor cells form large and well-demarcated tumors upon intracranial inoculation, we chose this *in vivo* orthotopic mouse model of GBM to test the targeted localization of EdU into tumor cells in the brain (26,27). Upon confirming tumor establishment via bioluminescent imaging (BLI), we randomized these mice into four different groups to be injected with PBS Control, 200 mg/kg EdU, 5 mg/kg TMZ, or 5 mg/kg TMZ + 200 mg/kg EdU. These injections were administered for 3 consecutive days, and the brains of mice were harvested the following day to perform hematoxylin and eosin (H&E), nuclear (DAPI) and EdU staining. In **Figure 2**, the presence of tumor mass is seen with H&E staining. Once the tumor cells were confirmed with H&E, EdU staining via click chemistry along with nuclear staining (DAPI) was performed on the slices from the same area of the brains. As negative controls, there was no EdU signal detected in either tumor or non-tumor cells in the brains of mice administered with PBS or 5 mg/kg TMZ, pointing out the specificity of EdU staining via click chemistry (**Fig 2A, 2B, 2E and 2F**). On the other hand, the EdU signal (green) was highly localized to the tumor cells in mice treated with both 200 mg/kg EdU (**Fig. 2C**) and 5 mg/kg TMZ + 200 mg/kg EdU (**Fig. 2D**). The quantification of EdU-positive cells in tumor versus non-tumor cells revealed ~83 times more EdU-positive cells in 200 mg/kg EdU-treated group and ~70 times more EdU positive cells in 5 mg/kg TMZ and 200 mg/kg EdU-treated group (**Fig. 2G, ****p<0.0001 for both comparisons**). The residual EdU signal observed in **Fig. 2C-2D** was localized mostly to the subventricular zone (SVZ) of the brain, which is known to harbor some proliferative cells (28). These results confirmed the highly targeted localization of EdU into tumor cells *in vivo*. To our knowledge, EdU's distribution in blood plasma and brain has not been characterized before. To characterize this biodistribution and clearance of EdU *in vivo*, we next performed a pharmacokinetic study with healthy female athymic nude mice. We administered a single dose of 200 mg/kg EdU, collected blood plasma and brain samples from mice at six different time points ranging from 15 mins to 6 hrs, and obtained the EdU concentration over time via LC-MS/MS (**Fig. 3A**). In plasma, the maximum concentration of EdU was reached at 15 minutes at ~73 μg/ml, with a half-life of ~10 minutes (**Fig. 3B**). On the other hand, in brain, the maximum concentration of EdU was reached at 15 minutes at ~4.8 μg/ml, with a half-life of ~30 minutes (**Fig. 3C**). The mean $AUC_{0-\infty}$ values for plasma and brain were 42.14 and 4.92, respectively, corresponding to a brain-to-plasma (B/P) AUC ratio of approximately 0.12 for EdU. Together, these results supported our hypothesis that EdU gets specifically localized into the tumor cells in the brain *in vivo* and identified the pharmacokinetic parameters of EdU in blood plasma and brain tissue for the first time.

Testing TMZ+EdU combination therapy *in vitro* in human GBM cells and *in vivo* in orthotopic mouse models of GBM

It has been found that combinations of various mutations in oncogenes and tumor suppressor genes give rise to GBM (5). Human GBM cell lines derived from patients are widely used in testing

141 drug candidates both *in vitro* and *in vivo*. To recapitulate this heterogeneous genetic profile, in our
142 study, we used 3 human GBM cell lines with different sets of mutations (27,29–34) in testing the
143 combination of TMZ and EdU: U87, GBM8, and LN229. All of these cell lines are engineered to
144 express firefly luciferase (FLuc) and thus bioluminescence signal measured upon incubation with
145 luciferin is used as a measure of viability. We tested these cell lines with the standard of care drug
146 TMZ and EdU, and the TMZ+EdU combination. Testing was done by cell survival assay *in vitro*
147 and by monitoring survival and tumor growth *in vivo* in female athymic nude mice bearing
148 orthotopic xenografts of these 3 cell lines.
149
150 ***Testing TMZ+EdU combination therapy in vitro in U87 cell line and in mice bearing***
151 ***orthotopic xenografts of U87***
152 We first tested for a potential synergistic effect of TMZ and EdU combination on U87 cells *in vitro*
153 before proceeding to *in vivo* with this cell line. We have reported the IC50 value of EdU for this
154 cell line as 40 μM (25). Cell survival assay with the combination of EdU at this concentration and
155 various doses of TMZ showed that these two drugs are synergistic, especially at the higher doses
156 of TMZ (**Fig. S1A**). This *in vitro* synergism between TMZ and EdU encouraged us to test this
157 combination *in vivo* in the mice bearing orthotopic xenografts of U87 cells.

158 To establish the *in vivo* orthotopic mouse model with the U87 cell line, we inoculated U87 cells
159 intracranially into the brain parenchyma of female athymic nude mice and confirmed
160 establishment of tumors via BLI. Informed by our results on the pharmacokinetic features of EdU,
161 we decided to administer EdU at 200 mg/kg every Monday-Friday at a once daily frequency and
162 TMZ at 5 mg/kg every Monday, Wednesday, and Friday once every other day for a total of 6
163 weeks. For the combination group, mice received the TMZ injections in the morning and EdU
164 injections in the afternoon with the indicated regimens for 6 weeks. Upon randomization of mice
165 into PBS control and three treatment groups on Day 7 (**Fig. S1B**), we monitored the tumor growth
166 of these mice via BLI. Neither 200 mg/kg EdU nor 5 mg/kg TMZ treatment showed a successful
167 suppression of tumor growth while the treatment with the combination of 200 mg/kg EdU and 5
168 mg/kg TMZ suppressed the tumor growth and decreased the tumor signal below the baseline
169 level (**Fig. 4A**). This suppression lasted as long as the injections continued. However, once the
170 injections were completed by Day 46, the tumors recurred in 7-10 days, and the mice started to
171 reach humane end point after ~15 days following the discontinuation of the treatment. **Figure 4B**
172 shows the BLI images of representative mice throughout the study (see **Fig. S1B-G** for extended
173 BLI images). While treatment with single-agent 200 mg/kg and 5 mg/kg TMZ extended the survival
174 by ~30% and ~50%, respectively, compared to the PBS control group ($p<0.0008$ and $p<0.0001$,
175 respectively), combination of 5 mg/kg TMZ and 200 mg/kg EdU extended the survival by more
176 than 130% compared to PBS control group ($p<0.0001$). Additionally, combination group extended
177 the survival by ~60% and ~80% compared to the single-agent TMZ and EdU groups, respectively
178 (**Fig. 3C,** $p<0.0001$ for both comparisons). At the study endpoint of this study, 1 out of 8 mice in
179 the combination group showed no detectable tumor BLI signal, and the brain of this mouse did
180 not show detectable tumor cells at or around the tumor cell inoculation site (**Fig. S1G-H**).
181 Moreover, at the study endpoint, ~%12 of mice (1 out of 8 mice) in 5 mg/kg TMZ + 200 mg/kg
182 EdU group was alive. Thus, we concluded that TMZ and EdU combination showed a synergistic
183 effect *in vivo* in suppressing the tumor growth and increasing the survival in mice bearing
184 orthotopic xenografts of U87 cells.
185
186 ***Testing the synergistic effect of TMZ and EdU combination in vitro in the GBM8 cell line***
187 ***and in mice bearing orthotopic xenografts of GBM8***
188 Upon obtaining these results with the U87 *in vivo* model, we moved on to test the potential
189 synergistic effect of the combination of TMZ and EdU on GBM8 cell line *in vitro*. Previously, the
190 IC50 value of EdU for this cell line was identified as ~50 nM (25). Cell survival assay combining

191 this IC50 value of EdU with various doses of TMZ showed synergistic to additive effect at the high
192 doses of TMZ (**Fig. S2A**). Although the synergism observed in GBM8 was not as high as that in
193 U87 in cell survival assay, it was encouraging enough to proceed with GBM8 cell line to establish
194 an *in vivo* orthotopic mouse model of GBM.

195 To this end, we started out by inoculating GBM8 cells intracranially into the brain parenchyma of
196 female athymic nude mice. After confirmation of tumor establishment via BLI, mice were
197 randomized into PBS control and treatment groups on Day 9 (**Fig. S2B**). Considering the inherent
198 sensitivity of GBM8 cell line to TMZ, we chose two different TMZ doses in this model; the first
199 being low dose (1 mg/kg) and the second being high dose (5 mg/kg). For the dose of EdU
200 treatment, we used 200 mg/kg again as in U87 *in vivo* model, considering the fast clearance of
201 the molecule. The combination groups featured combination of 1 mg/kg TMZ and 200 mg/kg and
202 the combination of 5 mg/kg TMZ and 200 mg/kg, separately. As in the U87 *in vivo* model, 6 weeks
203 of injections were administered with the M-F and MWF treatment regimens for EdU and TMZ,
204 respectively. Unlike the U87 *in vivo* model, following the end of 6 weeks of injections, we wanted
205 to investigate tumor recurrence and response to maintenance therapy in all treatment groups.
206 Thus, we set a recurrence criteria per mouse where treatment was resumed when the tumor's
207 BLI signal increased to ≥10× its baseline (initial) value and a discontinuation criteria per mouse
208 where reinjections were discontinued once the tumor's BLI signal returned to and stabilized at the
209 baseline level. The tumor growth was assessed via BLI in two phases: first phase during the
210 administration of 6 weeks of injections (Day 7 to Day 50) and the second phase during the
211 monitoring of tumor recurrence and response to as-needed maintenance therapy (Day 50 to study
212 endpoint, Day 170).

213 ***Assessment of tumor growth and recurrence during the first phase of treatment and the***
214 ***second phase of maintenance therapy in mice bearing orthotopic xenografts of GBM8***
215 During the first phase, we observed suppression of tumor growth in all mice except the ones that
216 received PBS and 1 mg/kg TMZ (**Fig. 5A**, **5C**, **S2B**, **S2C**, **S3A-F**). During the second phase, when
217 the initial treatment regimen had been discontinued, we started to observe recurrence in some
218 mice in the 5 mg/kg TMZ, 200 mg/kg EdU, and 1 mg/kg TMZ + 200 mg/kg EdU groups and
219 initiated maintenance therapy on recurrent mice on Days 59 and 63 (**Fig. 5B**, **S3B**, **S3C**, **S3F**).
220 Recurrence occurred in ~60% (4 out of 7) of mice in the 5 mg/kg TMZ group, 100% (6 out of 6)
221 of mice in the 200 mg/kg EdU group, and ~15% (1 out of 7) of mice in the 1 mg/kg TMZ + 200
222 mg/kg EdU group. In contrast, no recurrence was observed in any mice in the 5 mg/kg TMZ + 200
223 mg/kg EdU group (**Fig. 5B**, **S3D)**. According to the tumors' BLI signals, none of the recurred mice
224 in the 5 mg/kg TMZ group responded to maintenance therapy while 50% of the recurred mice in
225 the 200 mg/kg EdU group responded to maintenance therapy and showed remission (**Fig. 5B**,
226 **S3B**, **S3C**). One case of recurrence observed in the 1 mg/kg TMZ + 200 mg/kg EdU group also
227 showed suppression of tumor growth and eventually remission upon receiving maintenance
228 therapy (**Fig. 5B, 5C** and **S3F**; see **Fig. S2B-G** for extended BLI images). From these results, we
229 concluded that maintenance therapy with single-agent EdU and combination of TMZ and EdU
230 helped with suppressing the tumors while maintenance therapy with single-agent TMZ did not
231 provide any benefit in suppressing the tumors.
232
233 ***Monitoring survival in mice bearing orthotopic xenografts of GBM8***
234 In addition to assessing tumor growth and recurrence, we also monitored survival throughout the
235 study in the *in vivo* GBM8 model. At the study endpoint, single-agent treatments with 1 mg/kg
236 TMZ, 5 mg/kg TMZ, and 200 mg/kg EdU extended the survival significantly by ~10%, ~200%, and
237 ~260%, respectively, compared to the PBS control group (p=0.0037, p=0.0005 and p=0.0011,
238 respectively, **Fig. 5D**). Moreover, 50% of mice (3 out of 6 mice) in 200 mg/kg EdU group and
239 ~30% of mice (2 out of 7 mice) in 5 mg/kg TMZ group were alive by the study endpoint.

Importantly, all of the mice in 1 mg/kg TMZ + 200 mg/kg EdU and 5 mg/kg TMZ + 200 mg/kg combination groups were alive and tumor-free by the study endpoint, conferring a complete survival at the study endpoint in this stringent patient-derived model and highlighting the strong therapeutic potential of TMZ+EdU combination (**Fig. 5D**). We concluded from these results that the combination of TMZ and EdU conferred a synergistic effect in terms of both suppressing the tumor growth and extending the survival in mice bearing orthotopic xenografts of GBM8 cells. Combined with the results of the U87 *in vivo* model, these results supported our hypothesis that combining TMZ and EdU could yield a greater therapeutic effect than either of these drugs confers alone.

Testing TMZ+EdU combination therapy in vitro in LN229 cell line and in mice bearing orthotopic xenografts of LN229

Upon observing these synergistic results with the GBM8 *in vivo* model, we wished to test this synergistic effect in a third orthotopic *in vivo* model using LN229 cell line. Before establishing the *in vivo* orthotopic model with this cell line, we performed cell survival assay to test the synergistic effect of TMZ+EdU *in vitro* by combining the IC50 value of EdU for LN229 (~20 μM, as identified previously (25)) with various doses of TMZ. As in the other two GBM cell lines, the TMZ+EdU combination was more efficient than either drug alone at higher concentrations of TMZ (**Fig S4A**). These synergistic results led us to test the synergism of TMZ+EdU combination in the *in vivo* orthotopic model with LN229 cell line.

Accordingly, we created the *in vivo* orthotopic model by inoculating LN229 cells intracranially into the brain parenchyma of female athymic nude mice. Upon confirming the establishment of tumors via BLI, we stratified the mice into PBS control and five treatment groups on Day 4 (**Fig. S4B**). We chose the same treatment groups and treatment regimen with 6 weeks of injections as in the GBM8 *in vivo* model. By the third week of injections, mice in PBS control group started to reach humane end point while the tumors' BLI signals in all the other groups, except 200 mg/kg EdU group, decreased below the baseline level, indicating suppression of tumor growth (**Fig. 6A**, **6B**, **S4C**). On the other hand, 200 mg/kg EdU treatment was only able to stabilize the tumors' BLI signals at ~3 times the baseline level signal. By the completion of 6 weeks of injections on Day 46, all the mice in the PBS control group reached humane endpoint and the tumors' BLI signals in 200 mg/kg EdU groups started to increase. However, the tumors' BLI signals in TMZ single-agent and TMZ+EdU combination groups decreased further and stabilized ~0.01 times the baseline levels (**Fig. 6A**). Around a month after the completion of injections by Day 70, mice treated with 200 mg/kg EdU started to reach humane endpoint while tumors' BLI signals in combination or single-agent TMZ groups remained lower than the baseline level signal (**Fig. 6A**, **S4D-F**). Additionally, around Day 80 in 25% (2 out of 8 mice) of mice in 1 m/kg TMZ group and on Day 85 in ~12% (1 out of 8 mice) of mice in 5 mg/kg TMZ group, we started to observe some recurrence (**Fig. 6A**, **6B, S4G**). However, this recurrence was not observed in either of the combination groups. For survival, treatment with 200 mg/kg EdU extended the median survival significantly by ~110% compared to the PBS control group ($p=0.0002$, **Fig. 6C**). At conclusion of the study, none of the mice in 5 mg/kg TMZ + 200 mg/kg EdU group reached the humane endpoint, resulting in a striking and significant increase in median survival compared to both PBS control and single-agent EdU treatment groups ($p<0.0001$ and $p=0.0008$, respectively, **Fig.6C**). Similarly, 1 mg/kg TMZ + 200 mg/kg EdU group extended the survival significantly compared to both PBS control and single-agent EdU group ($p<0.0001$ and $p=0.0018$, respectively, **Fig.6C**). In 1 mg/kg TMZ + 200 mg/kg EdU group, only one mouse reached humane endpoint due to orbital infection, although its tumor had way lower BLI signal compared to the baseline level, corresponding to ~88% survival at the study endpoint. However, different from our results in U87 and GBM8 *in vivo* models, in the LN229 *in vivo* model, we observed that combination of TMZ and EdU performed as well as the single-agent TMZ groups, leading to an additive effect in

290 suppressing the tumor growth and prolonging the median survival (**Fig. 6C**). Collectively, the
291 results from our *in vivo* orthotopic mouse models of GBM established with U87, GBM8 and LN229
292 cells provided preclinical evidence that TMZ+EdU combination could elicit a synergistic to partly
293 additive effect in GBM, supporting the progression of this combination to early-phase clinical
294 testing.

295 **Toxicity profiling of mice treated with EdU, TMZ and their combination in *in vivo* orthotopic**
296 **mouse model of U87**

297 To assess treatment-associated toxicity, we collected peripheral organs (intestine, kidney, spleen,
298 and liver) from mice bearing orthotopic xenografts of U87 at the humane endpoint. Organs were
299 fixed, processed, paraffin-embedded, sectioned, and stained with hematoxylin and eosin (H&E).
300 Slides were histopathologically evaluated and scored for organ-specific signs of toxicity (**Fig. S5**).
301 In the small intestine of U87 tumor-bearing mice, minimal to mild crypt epithelial
302 necrosis/apoptosis was observed in 8 of 10 animals treated with 200 mg/kg EdU. Regenerative
303 activity, evidenced by increased mitotic figures, was also present in some animals. In mice treated
304 with 5 mg/kg TMZ + 200 mg/kg EdU, no overt crypt necrosis/apoptosis was seen, but increased
305 mitotic figures were detected in 2 of 5 animals, suggesting earlier crypt injury followed by
306 regeneration. These mice survived ~30 days longer than EdU-only animals, supporting the
307 interpretation that the intestinal epithelium had recovered from prior EdU-related injury. No crypt
308 changes were observed in mice treated with 5 mg/kg TMZ or PBS. The mild severity and evident
309 reversibility of the crypt epithelial injury indicate a non-adverse effect. In the kidney, minimal
310 multifocal cortical tubular epithelial degeneration/regeneration was noted in 2 of 10 EdU-treated
311 animals and 1 of 5 animals receiving the TMZ+EdU combination, but not in TMZ-only or PBS-
312 treated mice. As this lesion is a common background finding and may occur with general
313 debilitation, its low incidence and severity suggest a non-adverse, possibly incidental effect. In
314 the spleen, increased extramedullary hematopoiesis (EMH) was observed in 7 of 10 mice treated
315 with EdU and 4 of 5 mice treated with TMZ+EdU, but not in TMZ-only animals and only minimally
316 in 1 of 7 PBS controls. This finding is considered EdU-related and likely reflects bone marrow
317 suppression. Slight decreases in splenic lymphocyte cellularity were also seen in EdU- and
318 combination-treated mice; however, similar changes occurred in PBS controls, suggesting a
319 stress-related rather than treatment-specific effect. In the liver, no hepatocellular injury was
320 detected. Minor group differences in hepatocellular vacuolation were consistent with expected
321 diurnal variation in glycogen content (hepatocytes from animals euthanized earlier in the day
322 typically exhibit greater glycogen-associated vacuolation than those euthanized later) (35–38).
323 Overall, these observations demonstrate that EdU, alone or in combination with TMZ, induced
324 only mild and reversible histopathological changes in peripheral organs. This conclusion is also
325 supported by the recovery of body weight after treatment in mice bearing U87, GBM8, and LN229
326 tumors (**Fig. S6A-C**).

327 In addition to these toxicity profiling of the peripheral organs, we also wanted to test the effect of
328 the treatment with EdU, TMZ and their combination on complete blood counts. To this end, we
329 collected blood samples from mice bearing LN229 tumors on three different days: two of them
330 during the 6 weeks of injections (Day 16 and Day 30) and one after the completion of 6 weeks of
331 injections (Day 58). According to the results of complete blood counts, there were only minor and
332 reversible differences between the counts of White Blood Cells (WBCs), Lymphocytes (LYMPH),
333 Neutrophils (NEUT), Basophils (BASO), Eosinophils (EO), and Red Blood Cells (RBC) values in
334 PBS control group on Day 16 and in all the other groups. Additionally, for all the counts of these
335 different cells, the values in all groups were mainly at or above the normal lower limit values by
336 Day 58 (**Fig. S7A-F**). These results, together with the results on the histopathological and body
337 weight changes, further confirmed that EdU, alone or in combination with TMZ, induced mild,
338 transient, and reversible toxicity.

Testing TMZ+EdU combination therapy against living, passage-zero GBM patient tumor tissues *ex vivo*

Upon collecting these promising *in vivo* results, we proceeded to test the efficacy of TMZ+EdU on living, passage-zero GBM patient tissues seeded atop organotypic brain slice cultures (25,39,40). In our previous investigation of EdU as a potential therapeutic for GBM, we observed differential response across all patient tumors tested with monotherapy EdU or TMZ (25). In these new experiments, we observed a similar trend. We exposed four IDH-wild-type WHO-classified uncultured patient GBM tissues to single-agent EdU or TMZ as well as a combination of both compounds. 3 out of 4 of these tissue samples (PTS125, PTS152, and PTS153) were from patients who clinically showed rapid tumor progression after receiving TMZ.

During treatment, TMZ and/or EdU were added under the transwell membranes supporting each tumor-bearing OBSC and allowed to diffuse through the OBSCs and into the tumor cells. All tumors were treated with EdU and/or TMZ at doses of 0, 100, 250, and 1000μM. Combination therapy of [TMZ + EdU] was given at doses of [0, 0], [100, 100], [250, 250] and [500 μM, 500 μM]. Among the tissues tested, we observed several doses where EdU alone or in combination with TMZ performed better than TMZ alone (**Fig. 7A-D**). Using the Zero Interaction Potency (ZIP) Synergy score (41,42) that measures the difference between observed effects of a combinatorial regimen and expected effects if individual drugs are not interactive, we found that the effect of the combinatorial therapy ranged from additive (0 < ZIP < 10 in PT158, PT125, PT152) to synergistic (ZIP > 10 in PT153) (**Fig. 7E**).

GBM tumors have significant intra- and inter-tumoral heterogeneity; therapies that are effective for some patients may not be effective for others, and vice versa. We therefore tested EdU against two passage-zero patient GBM tissues in combination with a range of other FDA-approved chemotherapies. We chose carboplatin and lomustine because of their cell cycle-independent anti-tumor activity to complement EdU's hypothesized activity during the S-phase (43,44), and also because lomustine is frequently used as a control arm in trials and sometimes considered the standard of care after GBM progression (43,45). We chose etoposide because its mechanism of action through the stabilization of the topoisomerase II-DNA cleavage complex is very different from EdU's and may elicit different downstream compensatory mechanisms. It has also been well-tolerated in heavily pretreated patients with refractory gliomas (46,47). We also chose the poly (ADP-ribose) polymerase-1 inhibitor (PARPi) Olaparib because it is under investigation as a radio and chemosensitizer (48,49). As such, it might potentiate EdU's ability to target glioma stem cells (GSCs) which have upregulated PARP that promotes base excision repair and the repair of single-strand breaks in treated cancer cells (50).

To assess these exploratory combinatorial regimens, we first used doses previously determined to be close to the ED50 values of each single agent. We then combined these drugs with 1000 μM EdU. Across all drugs tested in combination, we observed more killing in the combination groups than when the drug was used alone (**Fig. 7F**, **7G**). Notably, at the same doses, each patient tissue responded differently to each drug. For instance, in PTS152, there was a 2.9-fold increase in tumor killing when EdU was added to etoposide, but just a 1.2 fold increase in PTS153, (**Fig. 7F**, **7G**), further highlighting the need for more personalized and patient-centric models that capture patient-to-patient heterogeneity.

DISCUSSION

As the most common primary malignancy of the central nervous system, GBM carries an extremely poor prognosis, with only ~7% of patients surviving five years after diagnosis (51–53). Therefore, there is an urgent need to develop new treatment modalities for GBM. Current efforts focus on investigating the therapeutic potential of integrating different drugs into combinatorial

388 treatments with TMZ, the first-line chemotherapeutic for GBM. However, despite trials and
389 preclinical studies with agents such as lomustine (54), bevacizumab (55), and PARP inhibitors
390 (56,57), none of these combinations have received FDA approval to date.
391
392 In this work, we demonstrated in (i) GBM cell lines *in vitro*, (ii) orthotopic mouse models of GBM
393 *in vivo*, and (iii) living, uncultured GBM patient tissues on OBSC that EdU shows a synergistic
394 effect in GBM when combined with TMZ. Moreover, for the first time, we characterized the
395 pharmacokinetic features of EdU and confirmed the targeted localization of EdU into GBM tumor
396 cells *in vivo* in both single-agent EdU-treated and combination-treated mice.
397
398 Our results on pharmacokinetic characteristics of EdU *in vivo* highlighted the fast clearance of
399 EdU with limited penetrance to the blood brain barrier and suggested that there is room for
400 improvement to modulate the bioavailability of EdU via formulation. Formulating EdU would
401 increase the bioavailability and in turn the penetrance of EdU to blood brain barrier, potentiating
402 the therapeutic effect we observed in combination with TMZ.
403
404 In our U87 *in vivo* model, we observed only a partial increase in survival with single-agent TMZ
405 and EdU while neither was able to suppress the tumor growth. However, combination of TMZ and
406 EdU showed a truly synergistic effect in this model by both suppressing the tumor growth and
407 extending the survival drastically. On the other hand, in our GBM8 *in vivo* model, single-agent
408 EdU and TMZ (5 mg/kg) treatments conferred considerable survival benefit compared to PBS
409 control group. Nevertheless, we also observed recurrence in these single-agent treatment groups
410 with partial to no response to maintenance therapy. For instance, we observed recurrence and no
411 response to maintenance therapy in ~60% of the mice treated with 5 mg/kg TMZ, reflecting the
412 acquired resistance following an initial positive response to TMZ treatment. Notably, this TMZ
413 resistance was overcome in mice treated with 5 mg/kg TMZ + 200 mg/kg EdU since no recurrence
414 was observed in these mice by the study endpoint. These results point out the power of TMZ+EdU
415 combination in targeting the TMZ-resistant tumors which is a prevalent occurrence in the clinic.
416
417 Surprisingly, in our third *in vivo* model with LN229, we observed that single-agent TMZ treatments
418 initially performed as well as the combination treatment groups, indicating an additive effect in this
419 model. However, both single-agent TMZ groups exhibited recurrence following the completion of
420 six weeks of injections. Combination groups in this LN229 model, on the other hand, were still
421 able to avoid this recurrence, similar to the results in GBM8 model while the survival benefit these
422 combination treatments conferred was not as drastic as in GBM8 model. The difference among
423 these different *in vivo* models of GBM could be attributed to the heterogeneous nature of this
424 disease and the differences among the genetic alterations harbored by these GBM cell lines.
425 Additionally, further *in vivo* studies in these and other models featuring various doses of EdU in
426 combination with TMZ could identify lower doses of EdU that could still show synergistic effect.
427
428 Furthermore, on our OBSC platform, TMZ+EdU acted in an additive or synergistic manner against
429 all four passage-zero patient tumor tissues. Notably, these findings demonstrate that the positive
430 interactions between EdU and TMZ extend beyond *in vitro* and animal models to actual
431 heterogeneous human tumors. The more muted responses measured here reflect what one may
432 expect to observe in the clinical setting, where tumors with heterogeneity in proliferation rate and
433 mutational drivers are typically not responsive to TMZ alone and respond incrementally to
434 combination therapies. The heterogeneity of patient-to-patient response also highlights the need
435 for more personalized and patient-centric models in drug development. Our OBSC platform may
436 therefore serve as a functional correlative biomarker to identify patients most likely to benefit from
437 TMZ+EdU or other combinatorial regimens. Expanding OBSC testing of EdU to a larger,

438 molecularly diverse cohort could refine the estimated prevalence of synergy, enable biomarker
439 discovery, and further advance functional precision medicine efforts in GBM.
440
441 **New therapeutic avenues to pursue: EdU's potential in combination with various other**
442 **chemotherapeutics**
443 Our results on combining EdU with various other chemotherapeutics against GBM patient tumor
444 tissues revealed the transformative role EdU could play in alternative treatment regimens for
445 GBM. By targeting complementary mechanisms of action in these combinations, we found
446 patient-specific sensitivities to different combination therapies. Future studies further testing the
447 mechanism and therapeutic potential of these combinatorial regimens will shed light on the clinical
448 utility of each in GBM. Introducing such personalized combination regimens into clinical GBM
449 treatment could provide much-needed alternatives for patients with GBM.
450
451 **MATERIALS & METHODS**
452 **Cell Lines**
453 U87 (purchased from ATCC in 2012, catalog #: HTB-14, RRID: CVCL_0022) and LN229
454 (purchased from ATCC in 2012, catalog #: CRL-2611, RRID: CVCL_0393) cells were cultured in
455 1X DMEM supplemented with 10% fetal bovine serum (FBS) and 1% penicillin-streptomycin in
456 T75 flasks. Patient-derived GBM8 cells (a kind gift from gift from H. Wakimoto, Massachusetts
457 General Hospital) (29,30) were cultured in neurobasal-A medium (Gibco, catalog #: 12349015)
458 supplemented with 1 mg heparin (STEMCELL Technologies, catalog #: 07980), 10 µg FGF
459 (Shenandoah Biotechnology, catalog #: 100-146), 10 mL B27 supplement (Life Technologies Inc.,
460 catalog #: A3582801), 7.5 mL L-glutamine (Life Technologies Inc., catalog #: 10888022), 10 µg
461 EGF (Shenandoah Biotechnology, catalog #: 100-26-100ug), 2.5 mL N2 supplement (Life
462 Technologies Inc., catalog #: 17502048), and 2.5 mL Antibiotic-Antimycotic (100X) (Thermo
463 Fisher Scientific, catalog #: 15240062) in T75 flasks.
464
465 **Lentiviral vectors**
466 The following lentiviral vector (LV) was used in this study: mCherry protein fused to firefly
467 luciferase (LV–mCh-FL). This LV also encodes a puromycin resistance gene. U87, GBM8 and
468 LN229 cell lines were transduced with this mCherry-FLuc Lentivirus. Following transduction,
469 mCherry expression was confirmed and cells expressing mCherry were selected using puromycin
470 treatment.
471
472 ***In vitro* survival assay via BLI**
473 The cells were counted using a Countess Cell Counter (Thermo Fisher Scientific, catalog #:
474 AMQAX1000) and seeded in triplicate with a 2500 cells/well density in black bottom 96 well plate.
475 Following 24 h incubation, the cells were treated with increasing doses of single agent TMZ
476 (Sigma-Aldrich, catalog #: T2577-100MG), single agent EdU (Sigma-Aldrich, catalog #: 900584-
477 500MG). For combination, IC50 value of the cell line for EdU was combined with increasing doses
478 of TMZ. At the end of 72 h treatment, the cell viability was measured via BLI using an AMI optical
479 imaging system. The data was analyzed using Aura software, Microsoft Excel, and GraphPad
480 Prism to plot dose-response curves ('Non-linear Regression (curve fit)' option used in GraphPad
481 Prism).
482
483 **Assessing synergism between TMZ and EdU *in vitro***
484 The cell viability data obtained from 3 biological replicates of *in vitro* survival assay via BLI of U87,
485 LN229 and GBM8 cell lines for each single dose of single agent EdU, TMZ or their combination
486 were fed in CompuSyn software as Fa (fraction affected). The CompuSyn software then
487 generated "Logarithmic Combination Index Plot" for drug combinations for each cell line where
488 log of Combination Index (CI) is plotted against the Fa (58–60). In this plot, the log(CI)<0,

log(CI)=0 and log(CI)>0 show synergism, additive effect and antagonism between EdU and TMZ, respectively.

Establishment of *in vivo* orthotopic xenograft mouse models of human GBM

All animal experiments were conducted in accordance with institutional guidelines and approved by the Institutional Animal Care and Use Committee (IACUC) at the University of North Carolina at Chapel Hill (UNC-CH) under UNC IACUC protocol 25-016. Female athymic nude mice (in-house bred) were housed under sterile conditions in an AAALAC-accredited animal facility at UNC-CH.

U87, LN229, and GBM8 glioma cells expressing luciferase were cultured and prepared for intracranial (i.c.) inoculation into the brains of athymic female nude mice. U87 and LN229 cells were detached using 0.05% Trypsin-EDTA (1X; Gibco, catalog #25300-054) and incubated for 5 minutes. GBM8 cells were detached using 1X Accutase (STEMCELL Technologies, catalog #: 07920) and incubated for 5 minutes, with declumping by pipetting at 2.5 minutes. After detachment, cells were counted using a Countess II Cell Counter, and suspensions were prepared in PBS at final concentrations of 3.3×10^4 cells/μL (U87), 5×10^4 cells/μL (GBM8), and 8.3×10^4 cells/μL (LN229). For intracranial inoculation, mice were anesthetized with isoflurane (2.0–2.5% for induction; 2.5–3.0% for maintenance) and placed in a stereotactic apparatus following confirmation of adequate anesthesia via a negative toe-pinch reflex. After surgical site preparation, a midline scalp incision was made (<10 mm) and a ~1 mm burr hole was drilled to facilitate needle insertion for intracranial injection. Each mouse was injected with a 3 μL volume of the corresponding cell suspension of U87, GBM8 or LN229 cells using the following coordinates relative to bregma: mediolateral (ML) = 2.5 mm, anteroposterior (AP) = 0.5 mm, dorsoventral (DV) = 2 mm. The total cells inoculated were 100,000 cells per mouse for U87 (n=40), 250,000 cells per mouse for LN229 (n=50), and 150,000 cells per mouse for GBM8 (n=42). The wounds were closed with 3M Vetbond™ tissue adhesive. Mice were monitored during and post-surgery and received meloxicam once daily for 48 hours postoperatively as established in the approved animal protocol.

Monitoring tumor growth via BLI in *in vivo* orthotopic xenograft mouse models of human GBM

Four to nine days post-implantation of U87, GBM8 or LN229 cells into the brains of mice, mice were injected with IVISbrite D-Luciferin Potassium Salt Bioluminescent Substrate (1g, XenoLight) (Revvity, catalog #: 122799-5) at 150 mg/kg, anesthetized with isoflurane and imaged via bioluminescence imaging (BLI) with IVIS Spectrum optical imaging system. The BLI signals recorded were analyzed using the LivingImage software and mice were stratified into treatment groups based on tumor burden as assessed by BLI. The monitoring of tumor growth in all of these *in vivo* models continued throughout the study durations at a frequency of 2-3 times a week.

Administration of EdU, Temozolomide (TMZ), and their combination, monitoring of tumor growth and evaluation of therapeutic response in *in vivo* orthotopic xenograft mouse models of human GBM

For the U87 and LN229 models, mice received a total of 6 weeks of injections. The treatment regimen for EdU was 200 mg/kg EdU once every weekday (M-F) and for TMZ either 1 mg/kg or 5 mg/kg TMZ every other weekday (MWF). For the combination group, the mice received TMZ injections in the morning and EdU injections in the afternoon with the same regimens. The tumor growth was monitored via bioluminescence imaging (BLI) of the mice using IVIS Spectrum device through intraperitoneally injecting luciferin. The mice started to receive treatment with EdU, TMZ and their combination 6 days and 4 days post tumor cell inoculation for U87 model and LN229 model, respectively. For the GBM8 model, the mice started to receive 6 weeks of injections with

538 the abovementioned regimens for EdU, TMZ and their combination 7 days post tumor cell
539 inoculation and the tumor growth was monitored similarly. Different from the other models, the
540 injections restarted once a mouse's tumor recurred in GBM8 model. The recurrence criterion was
541 recording a BLI signal that is 10 times higher than the initial signal recorded 7 days post tumor
542 cell inoculation. The injections continued until a consistently low BLI signal (4 BLI readings
543 showing either the same initial BLI signal or lower). The injections were discontinued once this
544 stopping criterion was met. Tumor growth was continuously monitored by BLI throughout the
545 duration of the studies in all models. In the U87 and LN229 models, mice underwent a 6-week
546 treatment regimen. EdU was administered at 200 mg/kg once daily on weekdays (Monday–
547 Friday), while TMZ was given at either 1 mg/kg or 5 mg/kg every other weekday (Monday,
548 Wednesday, Friday). For combination treatment, mice received TMZ injections in the morning and
549 EdU in the afternoon, following the same individual dosing schedules. Tumor growth was
550 monitored via bioluminescence imaging (BLI) using the IVIS Spectrum system, following
551 intraperitoneal injection of luciferin. Treatment began 6 days post–tumor cell inoculation for the
552 U87 model and 4 days post-inoculation for the LN229 model. In the GBM8 model, treatment also
553 began 7 days after tumor cell inoculation and followed the same 6-week regimen. Tumor
554 progression was monitored via BLI, as in the other models. Unique to GBM8, treatment resumed
555 upon tumor recurrence, defined as a BLI signal ≥10x the baseline signal recorded on day 7 post-
556 inoculation. Injections continued until the BLI signal returned to and remained at baseline or lower
557 for four consecutive readings, at which point treatment was discontinued. Tumor growth was
558 continuously monitored by BLI throughout the duration of the studies in all models, along with
559 survival tracking. Mice were also observed daily or every other day for signs of neurological
560 symptoms, ≥20% body weight loss, or decline in body condition score. Animals exhibiting any of
561 these signs were euthanized. Survival analysis was performed using the log-rank (Mantel–Cox)
562 test in GraphPad Prism.
563
564 **Blood collection from mice bearing orthotopic xenografts of LN229 cells for complete**
565 **blood counts**
566 Blood samples were obtained via a small venous nick on the mouse tail using a 22-gauge needle.
567 This procedure was performed on mice bearing orthotopic xenografts of LN229 cells and receiving
568 different treatment regimens and complete blood counts were assessed on days 16, 30, and 58
569 following tumor implantations. Blood collection volumes adhered strictly to the approved animal
570 use protocol. A maximum of three sampling sessions were conducted at bi-weekly intervals, with
571 each individual collection limited to approximately 30-50 µL. Complete blood counts (CBCs) were
572 performed on whole blood using an IDEXX ProCyte Dx™ Hematology Analyzer. Parameters
573 measured included indices of leukocyte, erythrocyte, and platelet lineages.
574
575 **Processing, embedding, sectioning, staining and imaging of tissues from peripheral**
576 **organs of mice bearing orthotopic xenografts of U87 and GBM8 Cells**
577 Formalin-fixed tissues were processed in a Leica Pegasus tissue processer, embedded in paraffin
578 (Leica Paraplast) using a HistoCore Arcadia H. Tissues were then sectioned on a microtome
579 (Leica, catalog #: RM2255) at 5 microns onto positively charged slides (Fisher Scientific, catalog
580 #: 12-550-15). For brains, the tissues were trimmed and sectioned around the site of tumor cell
581 inoculation in the right hemisphere at coordinates of 0.2 mm anterior-posterior (AP), 2.0 mm
582 mediolateral (ML), and 3.5 mm dorsoventral (DV).

583 **H&E staining and imaging**
584 Prior to H&E staining, slides were air dried overnight and baked for 30 minutes at 60 degrees
585 Celsius. H&E stains were performed using the Autostainer XL from Leica Biosystems. The slides
586 were deparaffinized in graded ethanol, then stained with Hematoxylin (Epredia, catalog #: 7211)
587 for 2 mins and Eosin -Y (Epredia, catalog #: 71311) for 1 min with respective washes in between.

588 Clarifier 2 (catalog #: 7402) and Bluing (catalog #: 7111) solutions from Epredia were used to
589 differentiate the reaction. After staining, slides were then dehydrated in graded ethanol, ending in
590 xylene, and coverslipped with Surgipath Micromount (Leica, catalog #: 3801731). Stained slides
591 were digitally imaged in the Aperio AT2 (Leica Microsystems) using 20x objective.

592 **EdU and DAPI staining and imaging**

593 The slides with brain tissues at the site of tumor inoculation were deparaffinized in graded ethanol.
594 They were then washed once with 1X Dulbecco's PBS (Gibco, catalog #: 14190144) for 10
595 minutes and once with 0.1% Triton X-100 (Sigma-Aldrich, catalog #: T9284-500ML) in PBS for 10
596 minutes in Coplin jars at room temperature. The slides were then permeabilized, blocked,
597 washed, and stained for EdU with Click-iT Plus Alexa Fluor picolyl azide toolkit (Thermo Fisher
598 Scientific, catalog #: C10641) and for DAPI with 1 µg/ mL Hoechst 33258, pentahydrate (bis-
599 benzimide) (Thermo Fisher Scientific, catalog #: H3569) as previously described (25). Upon
600 completion of these stainings, the slides were mounted with ProLong Gold Antifade Mountant
601 (Thermo Fisher Scientific, catalog #: P36934) and cured overnight.
602
603 The next day, slides were digitalized using the Aperio ScanScope FL (Aperio Technologies Inc).
604 The digital images were captured in each channel by 20x objective (0.468 µm/pixel resolution)
605 using line-scan camera technology (U.S. Patent 6,711,283). The adjacent 1 mm stripes captured
606 across the entire slide were aligned into a contiguous digital image by an image composer. Images
607 were archived in PSC's eSlide Manger database (Leica Biosystems).

608 **OBSC generation**

609 All animal work related to OBSC generation was approved by the Institutional Animal Care and
610 Use Committee at the University of North Carolina at Chapel Hill under protocol 22-171. P8
611 Sprague-Dawley rat pups were used for all OBSC preparation. Animals were housed with one
612 mother and no more than ten pups. All animals were euthanized prior to weaning. OBSCs were
613 generated as previously described**.** In brief, 300um coronal sections of rat brains were generated
614 with a VT1000S vibratome and suspended on a cell culture insert immersed in 1ml of brain slice
615 media consisting of "Neurobasal-A medium supplemented with 10% heat-inactivated pig serum,
616 5% heat-inactivated rat serum, 1 mM L-glutamine, 10 mM KCl, 10 mM HEPES, 1 mM sodium
617 pyruvate and 100 U/mL penicillin-streptomycin." (39,40) The slices were then incubated at 37°C,
618 5% CO2 and 95% humidity.

619
620 **Patient tissue identification, procurement, and processing**

621 All brain tumor specimens were collected at University of North Carolina Hospitals. A total of four
622 patients with primary or recurrent IDH-wild-type WHO-classified GBM diagnosis were included in
623 the present study. Appropriate written informed consent by parent/guardian and assent as
624 applicable was obtained under protocols where ethical approval was given by the Institutional
625 Review Board (IRB) in the Office of Human Research Ethics at the University of North Carolina
626 at Chapel Hill. All patients consented to non-interventional IRB Protocol #23-0834 (LCCC2212;
627 ClinicalTrials.gov NCT05978557), which began on 27/07/2023; estimated end date 01/03/2028.
628 The laboratory study team had no access to identifying patient information; de-identified or coded
629 diagnostic data describing tumor type and mutational status was provided by a Study Coordinator
630 or Honest Broker.

631 Upon standard of care surgery, leftover tumor tissues not necessary for diagnosis were
632 deidentified and transferred to the laboratory on wet ice. The tissue samples were immediately

633 washed with PBS and red blood cells (RBC) were lysed with an RBC lysis buffer. The tissue
634 samples were then mechanically dissociated with scalpels and cryopreserved at 150 mg of tissue
635 per ml of CryoStor CS10.
636
637 **Patient tissue processing and drug killing**
638 Originally cryopreserved patient tumor tissue samples were processed for drug dosing according
639 to established protocols at the Screening Live Cancer Explants Core Facility at UNC (25,39). In
640 brief, tissue samples were retrieved from liquid nitrogen storage, rapidly thawed, washed with
641 PBS and passed through a 100um strainer to approximate a single-cell suspension. The tissue
642 was then exposed to a LV–mCh-FL lentivirus to express both fluorescent mCherry and
643 bioluminescent firefly luciferase reporters. On Day 0, 1 mg of tissue was seeded atop each
644 hemisphere of brain slices suspended in a cell culture insert. On D1, corresponding doses of EdU,
645 TMZ, carboplation (Sigma Aldrich, catalog #: C2538-100MG), lomustine (Selleck Chemicals,
646 catalog #: S1840), Olaparib (Selleck Chemicals, catalog #: S1060), or etoposide (Sigma Aldrich,
647 E1383-100MG) diluted in 1 ml of brain slice media were added underneath the inserts. The treated
648 seeded tumors were then incubated for 3 days and bioluminescence readouts were obtained from
649 an AMI optical imaging system.
650
651 **Synergy score calculation**
652 All doses of drugs tested were exported into Synergy finder https://synergyfinder.org/ and synergy
653 scores were automatically calculated. Synergy scores less than -10, between -10 and +10, and
654 greater than +10 indicate antagonistic, additive, or synergistic interactions respectively.
655
656 **Pharmacokinetic Study**
657 Pharmacokinetic (PK) analyses were conducted in healthy 12-week-old female Nu/Nu mice. Each
658 animal received a single intraperitoneal (IP) dose of EdU (200 mg/kg). Blood and brain samples
659 were collected at 15 min, 30 min, 1 h, 2 h, and 4 h after the dose (n = 5 per time point) and at 6 h
660 (n = 3) under isoflurane anesthesia. Approximately 0.8–1.0 mL of blood was obtained via cardiac
661 puncture into K2EDTA tubes, immediately placed on ice, and centrifuged (5000 rpm, 5 min, 4 °C)
662 to obtain plasma. Brains were snap-frozen in liquid nitrogen. All samples were stored at −80 °C
663 until analysis.

664 **LC–MS/MS Quantification of EdU in Plasma and Brain**
665 For sample preparation, brains were weighed and diluted 1:2 with phosphate-buffered saline
666 (PBS), then homogenized using zirconium oxide beads in 2 mL tubes at 5000 RPM on a Precellys
667 24 homogenizer (VWR Bead Mill Homogenizer), applied twice for 20 seconds each.

668 Plasma (50 µL) or brain homogenate (diluted 1:1 with control plasma) was precipitated with
669 methanol containing D3-methotrexate (100 ng/mL) as the internal standard. After vortexing and
670 centrifugation (10,000 RPM, 10 min, 4 °C), 50 µL of the supernatant was diluted with 100 µL of
671 water for injection.

672 Liquid chromatography was performed on an Agilent 1260 Infinity II system equipped with a
673 Waters XSelect HSS T3 column (50 × 2.1 mm, 3.5 µm) at 30 °C. The mobile phases were (A)
674 water with 0.1% formic acid and (B) methanol with 0.1% formic acid. The gradient was 10% B (0–
675 1.0 min) to 50% B (3.0 min), returning to 10% B for a total run time of 7.0 min, at a flow rate of 0.2
676 mL/min. Injection volume was 4 µL.

677 Mass spectrometric detection used an Agilent 6470 triple quadrupole with AJS-ESI in positive-ion
678 MRM mode. The following transitions were monitored: m/z 253→136.9 (plasma) and 253→117
679 (tissue) for EdU, and m/z 458.2→311.2 for the internal standard. Quantification was performed

using peak-area ratios relative to matrix-matched calibration standards, following method validation.

Pharmacokinetic analysis

PK parameters were determined by non-compartmental analysis as described previously (61). Maximum plasma concentration (C_{max}) and time to maximum concentration (t_{max}) were derived directly from concentration-time profiles. The area under the concentration–time curve from 0 to 24 hours ($AUC_{0\text{-}24h}$) was calculated using the linear trapezoidal rule. The terminal elimination rate constant (kel) was obtained from the log-linear portion of the plasma concentration–time curve, and the elimination half-life ($t_{1/2}$) was calculated as $\ln 2/k_{el.}$ The area under the curve extrapolated to infinity ($AUC_{0-\infty}$) was determined as AUC_{0-24h} + ($C_{24h/kel}$). Apparent clearance (CL/F) was calculated as Dose/AUC_{total}, and apparent volume of distribution (Vd/F) as (CL/F)/k_{el}.

Acknowledgements:

We wish to thank UNC Pathology Services Core (PSC) and **Nicholas Pankow** in the UNC PSC for expert technical assistance with Histopathology and Digital Pathology. The UNC PSC is supported in part by an NCI Center Core Support Grant (P30CA016086). We also thank **Dr. Rani Suzanne Sellers** for expert assistance with toxicity scoring of peripheral organs and histopathologic review of brain and peripheral organs. All experiments using passage-zero patient tumor tissues was completed within the Screening Live Cancer Explants Core Facility at UNC. This research is supported by the National Center for Advancing Translational Sciences through NC TraCS (K12TR004416), and National Institute of Health (NIH) Grants ES033414 and GM118102. H.K. is supported by Fulbright PhD Grant. We would like to also extend our thanks to UNC Biomedical Research Imaging Center, UNC Advanced Translational Pharmacology and Analytical Chemistry (ATPAC) Core, UNC Animal Clinical Chemistry Core, and UNC SLiCE Core.

REFERENCES

1. Stupp R, Mason WP, van den Bent MJ, Weller M, Fisher B, Taphoorn MJB, et al. Radiotherapy plus concomitant and adjuvant temozolomide for glioblastoma. N Engl J Med. 2005 Mar 10;352(10):987–96.

2. Rong L, Li N, Zhang Z. Emerging therapies for glioblastoma: current state and future directions. J Exp Clin Cancer Res. 2022 Apr 15;41(1):142.

3. Singh S, Dey D, Barik D, Mohapatra I, Kim S, Sharma M, et al. Glioblastoma at the crossroads: current understanding and future therapeutic horizons. Signal Transduct Target Ther. 2025 Jul 9;10(1):213.

4. Sipos D, Raposa BL, Freihat O, Simon M, Mekis N, Cornacchione P, et al. Glioblastoma: Clinical Presentation, Multidisciplinary Management, and Long-Term Outcomes. Cancers (Basel). 2025 Jan 5;17(1).

5. Haque A, Banik NL, Ray SK. Molecular alterations in glioblastoma: potential targets for immunotherapy. Prog Mol Biol Transl Sci. 2011;98:187–234.

6. Radaelli E, Ceruti R, Patton V, Russo M, Degrassi A, Croci V, et al. Immunohistopathological and neuroimaging characterization of murine orthotopic xenograft models of glioblastoma multiforme recapitulating the most salient features of human disease. Histol Histopathol. 2009 Jul;24(7):879–91.

7. Davis ME. Glioblastoma: overview of disease and treatment. Clin J Oncol Nurs. 2016 Oct 1;20(5 Suppl):S2-8.

8. Hanif F, Muzaffar K, Perveen K, Malhi SM, Simjee SU. Glioblastoma Multiforme: A Review of its Epidemiology and Pathogenesis through Clinical Presentation and Treatment. Asian Pac J Cancer Prev. 2017 Jan 1;18(1):3–9.

9. Goenka A, Tiek D, Song X, Huang T, Hu B, Cheng S-Y. The many facets of therapy resistance and tumor recurrence in glioblastoma. Cells. 2021 Feb 24;10(3).

10. Silver DJ, Lathia JD. Therapeutic injury and tumor regrowth: tumor resection and radiation establish the recurrent glioblastoma microenvironment. EBioMedicine. 2018 May;31:13–4.

11. Rapp M, Baernreuther J, Turowski B, Steiger H-J, Sabel M, Kamp MA. Recurrence pattern analysis of primary glioblastoma. World Neurosurg. 2017 Jul;103:733–40.

12. Jiang H, Yu K, Li M, Cui Y, Ren X, Yang C, et al. Classification of progression patterns in glioblastoma: analysis of predictive factors and clinical implications. Front Oncol. 2020 Nov 3;10:590648.

13. Kawauchi D, Ohno M, Honda-Kitahara M, Miyakita Y, Takahashi M, Yanagisawa S, et al. Clinical characteristics and prognosis of Glioblastoma patients with infratentorial recurrence. BMC Neurol. 2023 Jan 7;23(1):9.

14. Yoon N, Kim H-S, Lee JW, Lee E-J, Maeng L-S, Yoon WS. Targeted genomic sequencing reveals different evolutionary patterns between locally and distally recurrent glioblastomas. Cancer Genomics Proteomics. 2020;17(6):803–12.

15. Wang L, Jung J, Babikir H, Shamardani K, Jain S, Feng X, et al. A single-cell atlas of glioblastoma evolution under therapy reveals cell-intrinsic and cell-extrinsic therapeutic targets. Nat Cancer. 2022 Dec 20;3(12):1534–52.

16. Chehade G, Lawson TM, Lelotte J, Daoud L, Di Perri D, Whenham N, et al. Long-term survival in patients with IDH-wildtype glioblastoma: clinical and molecular characteristics. Acta Neurochir (Wien). 2023 Apr;165(4):1075–85.

17. Lindsey-Boltz LA, Sancar A. New biochemical approaches for treatment of glioblastoma. J Biol Chem. 2025 Sep 20;110748.

18. Fantoni NZ, El-Sagheer AH, Brown T. A Hitchhiker's Guide to Click-Chemistry with Nucleic Acids. Chem Rev. 2021 Jun 23;121(12):7122–54.

19. Salic A, Mitchison TJ. A chemical method for fast and sensitive detection of DNA synthesis in vivo. Proc Natl Acad Sci USA. 2008 Feb 19;105(7):2415–20.

20. Zeng C, Pan F, Jones LA, Lim MM, Griffin EA, Sheline YI, et al. Evaluation of 5-ethynyl-2'-deoxyuridine staining as a sensitive and reliable method for studying cell proliferation in the adult nervous system. Brain Res. 2010 Mar 10;1319:21–32.

21. Maltsev DI, Mellanson KA, Belousov VV, Enikolopov GN, Podgorny OV. The bioavailability time of commonly used thymidine analogues after intraperitoneal delivery in mice: labeling kinetics in vivo and clearance from blood serum. Histochem Cell Biol. 2022 Feb;157(2):239–50.

22. Wang L, Cao X, Yang Y, Kose C, Kawara H, Lindsey-Boltz LA, et al. Nucleotide excision repair removes thymidine analog 5-ethynyl-2'-deoxyuridine from the mammalian genome. Proc Natl Acad Sci USA. 2022 Aug 30;119(35):e2210176119.

23. Ross HH, Rahman M, Levkoff LH, Millette S, Martin-Carreras T, Dunbar EM, et al. Ethynyldeoxyuridine (EdU) suppresses in vitro population expansion and in vivo tumor progression of human glioblastoma cells. J Neurooncol. 2011 Dec;105(3):485–98.

24. Ligasová A, Strunin D, Friedecký D, Adam T, Koberna K. A fatal combination: a thymidylate synthase inhibitor with DNA damaging activity. PLoS ONE. 2015 Feb 11;10(2):e0117459.

25. Kaanoglu H, Adefolaju A, Fraley C, Shobande M, Dasari R, Mann B, et al. Repurposing the DNA Labeling Agent EdU for Therapy against Heterogeneous Patient Glioblastoma. Mol Cancer Ther. 2025 Aug 1;24(8):1213–25.

26. Han J-H, Yoon JS, Chang D-Y, Cho KG, Lim J, Kim S-S, et al. CXCR4-STAT3 Axis Plays a Role in Tumor Cell Infiltration in an Orthotopic Mouse Glioblastoma Model. Mol Cells. 2020 Jun 30;43(6):539–50.

27. Schulz JA, Rodgers LT, Kryscio RJ, Hartz AMS, Bauer B. Characterization and comparison of human glioblastoma models. BMC Cancer. 2022 Aug 3;22(1):844.

794 28. Faiz M, Acarin L, Castellano B, Gonzalez B. Proliferation dynamics of germinative zone
795 cells in the intact and excitotoxically lesioned postnatal rat brain. BMC Neurosci. 2005 Apr
796 12;6:26.

797 29. Sasportas LS, Kasmieh R, Wakimoto H, Hingtgen S, van de Water JAJM, Mohapatra G,
798 et al. Assessment of therapeutic efficacy and fate of engineered human mesenchymal stem
799 cells for cancer therapy. Proc Natl Acad Sci USA. 2009 Mar 24;106(12):4822–7.

800 30. Wakimoto H, Kesari S, Farrell CJ, Curry WT, Zaupa C, Aghi M, et al. Human glioblastoma-
801 derived cancer stem cells: establishment of invasive glioma models and treatment with
802 oncolytic herpes simplex virus vectors. Cancer Res. 2009 Apr 15;69(8):3472–81.

803 31. Sullivan JP, Nahed BV, Madden MW, Oliveira SM, Springer S, Bhere D, et al. Brain tumor
804 cells in circulation are enriched for mesenchymal gene expression. Cancer Discov. 2014
805 Nov;4(11):1299–309.

806 32. Sesen J, Dahan P, Scotland SJ, Saland E, Dang V-T, Lemarié A, et al. Metformin inhibits
807 growth of human glioblastoma cells and enhances therapeutic response. PLoS ONE. 2015
808 Apr 13;10(4):e0123721.

809 33. DepMap Cell Line Summary [Internet]. [cited 2025 Oct 14]. Available from:
810 https://depmap.org/portal/cell_line/ACH-000075?utm_source=chatgpt.com&tab=overview

811 34. Ishii N, Maier D, Merlo A, Tada M, Sawamura Y, Diserens A-C, et al. Frequent Co-
812 Alterations ofTP53, p16/CDKN2A, p14 ,PTEN Tumor Suppressor Genes in Human Glioma
813 Cell Lines. Brain Pathol. 1999 Jul;9(3):469–79.

814 35. Liver, Hepatocyte - Glycogen Accumulation and Depletion - Nonneoplastic Lesion Atlas
815 [Internet]. [cited 2025 Oct 14]. Available from:
816 https://ntp.niehs.nih.gov/atlas/nnl/hepatobiliary-system/liver/Hepatocyte-
817 GlycogenAccumulationandDepletion?utm_source=chatgpt.com

818 36. Fuller RW, Diller ER. Diurnal variation of liver glycogen and plasma free fatty acids in rats
819 fed ad libitum or single daily meal. Metab Clin Exp. 1970 Mar;19(3):226–9.

820 37. Rothacker DL, Kanerva RL, Wyder WE, Alden CL, Maurer JK. Effects of variation of
821 necropsy time and fasting on liver weights and liver components in rats. Toxicol Pathol.
822 1988;16(1):22–6.

823 38. Wells MY, Weisbrode SE, Maurer JK, Capen CC, Bruce RD. Variable hepatocellular
824 vacuolization associated with glycogen in rabbits. Toxicol Pathol. 1988;16(3):360–5.

825 39. Mann B, Zhang X, Bell N, Adefolaju A, Thang M, Dasari R, et al. A living ex vivo platform
826 for functional, personalized brain cancer diagnosis. Cell Rep Med. 2023 Jun
827 20;4(6):101042.

828 40. Satterlee AB, Dunn DE, Lo DC, Khagi S, Hingtgen S. Tumoricidal stem cell therapy
829 enables killing in novel hybrid models of heterogeneous glioblastoma. Neuro Oncol. 2019
830 Dec 17;21(12):1552–64.

831 41. Yadav B, Wennerberg K, Aittokallio T, Tang J. Searching for Drug Synergy in Complex
832 Dose-Response Landscapes Using an Interaction Potency Model. Comput Struct
833 Biotechnol J. 2015 Sep 25;13:504–13.

42. Ianevski A, He L, Aittokallio T, Tang J. SynergyFinder: a web application for analyzing drug combination dose-response matrix data. Bioinformatics. 2017 Aug 1;33(15):2413–5.

43. Weller M, Le Rhun E. How did lomustine become standard of care in recurrent glioblastoma? Cancer Treat Rev. 2020 Jul;87:102029.

44. Bristol-Myers Squibb Company. Paraplatin(carboplatin) [package insert] [Internet]. 2010 [cited 2025 Oct 16]. Available from: https://www.accessdata.fda.gov/drugsatfda_docs/label/2010/020452s005lbl.pdf

45. Zeyen T, Treiber A, Schneider M, Potthoff A-L, Schaub C, Roever L, et al. Second-line temozolomide in first recurrent MGMT-methylated glioblastoma after lomustine/temozolomide: Efficacy and safety. Neurooncol Adv. 2025 Apr 28;7(1):vdaf084.

46. Reyhanoglu G, Tadi P. Etoposide. StatPearls. Treasure Island (FL): StatPearls Publishing; 2025.

47. van der Meulen M, Chahal M, Mason WP. The value of etoposide for recurrent glioma. Can J Neurol Sci. 2024 Jul;51(4):509–12.

48. Dhanavath N, Bisht P, Jamadade MS, Murti K, Wal P, Kumar N. Olaparib: A chemosensitizer for the treatment of glioblastoma. Mini Rev Med Chem. 2025;25(5):374–85.

49. Hanna C, Kurian KM, Williams K, Watts C, Jackson A, Carruthers R, et al. Pharmacokinetics, safety, and tolerability of olaparib and temozolomide for recurrent glioblastoma: results of the phase I OPARATIC trial. Neuro Oncol. 2020 Dec 18;22(12):1840–50.

50. Lesueur P, Lequesne J, Grellard J-M, Dugué A, Coquan E, Brachet P-E, et al. Phase I/IIa study of concomitant radiotherapy with olaparib and temozolomide in unresectable or partially resectable glioblastoma: OLA-TMZ-RTE-01 trial protocol. BMC Cancer. 2019 Mar 4;19(1):198.

51. Kaina B. Temozolomide, procarbazine and nitrosoureas in the therapy of malignant gliomas: update of mechanisms, drug resistance and therapeutic implications. J Clin Med. 2023 Nov 30;12(23).

52. Slika H, Karimov Z, Alimonti P, Abou-Mrad T, De Fazio E, Alomari S, et al. Preclinical models and technologies in glioblastoma research: evolution, current state, and future avenues. Int J Mol Sci. 2023 Nov 14;24(22).

53. Price M, Ballard C, Benedetti J, Neff C, Cioffi G, Waite KA, et al. CBTRUS Statistical Report: Primary Brain and Other Central Nervous System Tumors Diagnosed in the United States in 2017-2021. Neuro Oncol. 2024 Oct 6;26(Supplement_6):vi1–85.

54. Herrlinger U, Tzaridis T, Mack F, Steinbach JP, Schlegel U, Sabel M, et al. Lomustine-temozolomide combination therapy versus standard temozolomide therapy in patients with newly diagnosed glioblastoma with methylated MGMT promoter (CeTeG/NOA-09): a randomised, open-label, phase 3 trial. Lancet. 2019 Feb 16;393(10172):678–88.

55. Chinot OL, Wick W, Mason W, Henriksson R, Saran F, Nishikawa R, et al. Bevacizumab plus radiotherapy-temozolomide for newly diagnosed glioblastoma. N Engl J Med. 2014 Feb 20;370(8):709–22.

56. Jones AB, Tuy K, Hawkins CC, Quinn CH, Saad J, Gary SE, et al. Temozolomide and the PARP Inhibitor Niraparib Enhance Expression of Natural Killer Group 2D Ligand ULBP1 and Gamma-Delta T Cell Cytotoxicity in Glioblastoma. Cancers (Basel). 2024 Aug 15;16(16).

57. Yuan AL, Ricks CB, Bohm AK, Lun X, Maxwell L, Safdar S, et al. ABT-888 restores sensitivity in temozolomide resistant glioma cells and xenografts. PLoS ONE. 2018 Aug 28;13(8):e0202860.

58. Chou T-C, Talalay P. Quantitative analysis of dose-effect relationships: the combined effects of multiple drugs or enzyme inhibitors. Adv Enzyme Regul. 1984 Jan;22:27–55.

59. Chou: ComboSyn Inc; Paramus,(NJ): 2005 - Google Scholar [Internet]. [cited 2025 Oct 12]. Available from: https://scholar.google.com/scholar_lookup?title=ComboSyn%20Inc%20Paramus%20NJ&author=TC%20Chou&author=N%20Martin&publication_year=2005&

60. Chou T-C. Drug combination studies and their synergy quantification using the Chou-Talalay method. Cancer Res. 2010 Jan 15;70(2):440–6.

61. Akyel YK, Seyhan NO, Gül Ş, Çelik M, Taşkın AC, Selby CP, et al. The impact of circadian rhythm disruption on oxaliplatin tolerability and pharmacokinetics in Cry1-/-Cry2-/- mice under constant darkness. Arch Toxicol. 2025 Apr;99(4):1417–29.

906

907

908 **FIGURE LEGENDS**

909 **Figure 1:** Chemical structures of temozolomide **(A)** and 5-ethynyl-2'-deoxyuridine (EdU) **(B)**.

910 **Figure 2: Targeted localization of EdU into GBM tumor cells *in vivo* in single-agent EdU-**
911 **and TMZ+EdU combination-treated mice**. Hematoxylin and eosin (H&E), nuclear (DAPI), EdU
912 staining, and merged DAPI and EdU staining pictures in the brains of PBS- **(A)**, 5 mg/kg TMZ-
913 **(B)**, 200 mg/kg EdU- **(C)**, and 5 mg/kg TMZ + 200 mg/kg EdU-treated **(D)** mice bearing orthotopic
914 xenografts of U87. **(E)** Quantification of EdU-positive cells in non-tumor cells in the brains of PBS-
915 (n=4), 200 mg/kg EdU- (n=4), 5 mg/kg TMZ- (n=4), and 5 mg/kg TMZ + 200 mg/kg EdU-treated
916 (n=4) mice bearing orthotopic xenografts of U87 (One-way ANOVA, ****$p<0.0001$). **(F)**
917 Quantification of EdU-positive cells in tumor cells in the brains of PBS- (n=4), 200 mg/kg EdU-
918 (n=4), 5 mg/kg TMZ- (n=4), and 5 mg/kg TMZ + 200 mg/kg EdU-treated (n=4) mice bearing
919 orthotopic xenografts of U87 (One-way ANOVA, ****$p<0.0001$). **(G)** Quantification of EdU-positive
920 cells in tumor versus non-tumor cells in the brains of 200 mg/kg EdU- (n=4) and 5 mg/kg TMZ +
921 200 mg/kg EdU-treated (n=4) mice bearing orthotopic xenografts of U87 (Unpaired, two-tailed t-
922 test, ****$p<0.0001$).

923 **Figure 3: Pharmacokinetic features of EdU in blood plasma and brain. (A)** Overview of the
924 sample collection and analysis to identify pharmacokinetic parameters of EdU in blood plasma
925 and brain of female athymic nude mice. **(B)** EdU concentration versus time curve in blood plasma,
926 and Area Under Curve (AUC), maximum concentration (C_{max}), time to reach maximum
927 concentration (t_{max}), half-life ($t_{1/2}$), apparent clearance (CL/F) and volume of distribution (V_d)
928 parameters for EdU in blood plasma. **(C)** EdU concentration versus time curve in brain, and Area
929 Under Curve (AUC), maximum concentration (C_{max}), time to reach maximum concentration (t_{max}),
930 and half-life ($t_{1/2}$) parameters for EdU in brain.

931 **Figure 4: Testing the efficacy of TMZ+EdU in *in vivo* orthotopic U87 mouse model of GBM.**
932 **(A)** Bioluminescence imaging (BLI) signal fold changes of the tumors of mice bearing orthotopic
933 xenografts of U87 and treated with either PBS (n=8), 200 mg/kg EdU (n=8), 5 mg/kg TMZ (n=8),
934 or 5 mg/kg TMZ + 200 mg/kg EdU (n=8). Arrows under the x axis denote the days on which six
935 weeks of EdU and TMZ injections were administered. **(B)** Representative BLI images of mice
936 treated with either PBS, 200 mg/kg EdU, 5 mg/kg TMZ, or 5 mg/kg TMZ + 200 mg/kg EdU on
937 Days 7, 23, 31, 38, and 58. **(C)** Kaplan Meier survival plot of mice bearing orthotopic xenografts
938 of U87 and treated with either PBS, 200 mg/kg EdU, 5 mg/kg TMZ, or 5 mg/kg TMZ + 200 mg/kg
939 EdU (log-rank test).

940 **Figure 5: Testing the efficacy of TMZ+EdU in *in vivo* orthotopic GBM8 mouse model of**
941 **GBM. (A)** Bioluminescence imaging (BLI) signal fold changes of the tumors of mice bearing
942 orthotopic xenografts of GBM8 and treated with either PBS (n=5), 200 mg/kg EdU (n=6), 5 mg/kg
943 TMZ (n=7), 5 mg/kg TMZ + 200 mg/kg EdU (n=7), 1 mg/kg TMZ (n=6), or 1 mg/kg TMZ + 200
944 mg/kg EdU (n=7) during the first phase of treatment (day 0 to Day 50). Arrows under the x axis
945 denote the days on which six weeks of EdU and TMZ injections were administered. **(B)**
946 Bioluminescence imaging (BLI) signal fold change of the tumors of mice bearing orthotopic
947 xenografts of GBM8 and treated with either PBS (n=5), 200 mg/kg EdU (n=6), 5 mg/kg TMZ (n=7),
948 5 mg/kg TMZ + 200 mg/kg EdU (n=7), 1 mg/kg TMZ (n=6), or 1 mg/kg TMZ + 200 mg/kg EdU
949 (n=7) during the second phase of maintenance therapy (day 50 to Day 170). Arrows on the graph
950 denote the day of the initiation of maintenance therapy in corresponding color-coded group. **(C)**
951 Representative BLI images of mice bearing orthotopic xenografts of GBM8 and treated with either
952 PBS, 200 mg/kg EdU, 5 mg/kg TMZ, 5 mg/kg TMZ + 200 mg/kg EdU, 1 mg/kg TMZ, or 1mg/kg
953 TMZ + 200 mg/kg EdU on Days 9, 42, 133, and 168. **(D)** Kaplan Meier survival plot of mice bearing

954 orthotopic xenografts of GBM8 and treated with either PBS, 200 mg/kg EdU, 5 mg/kg TMZ, 5
955 mg/kg TMZ + 200 mg/kg EdU, 1 mg/kg TMZ, or 1mg/kg TMZ + 200 mg/kg EdU (log-rank test).

956 **Figure 6: Testing the efficacy of TMZ+EdU in *in vivo* orthotopic LN229 mouse model of**
957 **GBM. (A)** Bioluminescence imaging (BLI) signal fold changes of the tumors of mice bearing
958 orthotopic xenografts of LN229 and treated with either PBS (n=7), 200 mg/kg EdU (n=7), 5 mg/kg
959 TMZ (n=8), 5 mg/kg TMZ + 200 mg/kg EdU (n=8), 1 mg/kg TMZ (n=7), or 1 mg/kg TMZ + 200
960 mg/kg EdU (n=8). Arrows under the x axis denote the days on which six weeks of EdU and TMZ
961 injections were administered. **(B)** Representative BLI images of mice treated with either PBS, 200
962 mg/kg EdU, 5 mg/kg TMZ, 5 mg/kg TMZ + 200 mg/kg EdU, 1 mg/kg TMZ, or 1 mg/kg TMZ + 200
963 mg/kg EdU on Days 4, 24, 70, and 98. **(C)** Kaplan Meier survival plot of mice bearing orthotopic
964 xenografts of LN229 and treated with either PBS, 200 mg/kg EdU, 5 mg/kg TMZ, 5 mg/kg TMZ +
965 200 mg/kg EdU, 1 mg/kg TMZ, or 1 mg/kg TMZ + 200 mg/kg EdU (log-rank test).

966 **Figure 7: Testing the efficacy of TMZ+EdU in living, uncultured GBM patient tissues seeded**
967 **on OBSC.** Dose-response curves and grouped dose-response bar graphs of GBM patient tissues
968 PT153 **(A)**, PT158 **(B)**, PT125 **(C)**, and PT152 **(D)** treated with single-agent EdU, TMZ or
969 TMZ+EdU (Two-way ANOVA, ****p<0.0001, ***p<0.001). **(E)** Zero Interaction Potency (ZIP)
970 Synergy Score values and ZIP p values for TMZ+EdU combination tested on four GBM patient
971 tissues. High-throughput combo screening of PT153 **(F)** and PT153 **(G)** with 1000 μM EdU in
972 combination with carboplatin (50 μM), etoposide (10 μM), lomustine (250 μM), Olaparib (10 μM),
973 and TMZ (2000 μM).

974 **Figure S1: Testing the synergism of TMZ+EdU *in vitro* in U87 cell line, extended BLI images**
975 **and H&E staining on the brains of mice bearing orthotopic xenografts of U87 cells. (A)** Cell
976 survival assay via BLI and CompuSyn assessment of synergy with combination index (CI) values
977 on U87 cell line with the combination of 40 μM EdU (IC50 for U87) and various doses of TMZ
978 (log(CI)<0, log(CI)=0 and log(CI)>0 show synergism, additive effect and antagonism between
979 EdU and TMZ, respectively). Extended BLI images of mice bearing orthotopic xenografts of U87
980 cells on Days 7 **(B)**, 21 **(C)**, 31 **(D)**, 38 **(E)**, 48 **(F)**, and 58 **(G)**. **(H, I)** H&E staining showing no
981 detectable tumor on the brains of 2 surviving mice from the 5 mg/kg TMZ + 200 mg/kg EdU
982 treatment group.

983 **Figure S2: Testing the synergism of TMZ+EdU *in vitro* in GBM8 cell line, extended BLI**
984 **images of mice bearing orthotopic xenografts of GBM8 Cells. (A)** Cell survival assay via BLI
985 and CompuSyn assessment of synergy with combination index (CI) values on GBM8 cell line with
986 the combination of 50 nM EdU (IC50 for GBM8) and various doses of TMZ (log(CI)<0, log(CI)=0
987 and log(CI)>0 show synergism, additive effect and antagonism between EdU and TMZ,
988 respectively). Extended BLI images of mice bearing orthotopic xenografts of GBM8 cells on Days
989 9 **(B)**, 42 **(C)**, 94 **(D)**, 133 **(E)**, 150 **(F)**, and 168 **(G)**.

990 **Figure S3:** Spaghetti plots of bioluminescence imaging (BLI) signal fold changes of the tumors of
991 mice bearing orthotopic xenografts of GBM8 and treated with either PBS (n=5) **(A)**, 200 mg/kg
992 EdU (n=6) **(B)**, 5 mg/kg TMZ (n=7) **(C)**, 5 mg/kg TMZ + 200 mg/kg EdU (n=7) **(D)**, 1 mg/kg TMZ
993 (n=6) **(E)**, or 1 mg/kg TMZ + 200 mg/kg EdU (n=7) **(F)**.

994 **Figure S4: Testing the synergism of TMZ+EdU *in vitro* in LN229 cell line and extended BLI**
995 **images of mice bearing orthotopic xenografts of LN229 Cells. (A)** Cell survival assay via BLI
996 and CompuSyn assessment of synergy with combination index (CI) values on LLN229 cell line
997 with the combination of 20 μM EdU (IC50 for LN229) and various doses of TMZ (log(CI)<0,
998 log(CI)=0 and log(CI)>0 show synergism, additive effect and antagonism between EdU and TMZ,
999 respectively). Extended BLI images of mice bearing orthotopic xenografts of GBM8 cells on Days
1000 4 **(B)**, 24 **(C)**, 64 **(D)**, 70 **(E)**, 73 **(F)**, and 98 **(G)**.

1001 **Figure S5: Toxicity profiling of the mice bearing orthotopic xenografts of U87 cells.**
1002 Summary of toxicity findings on the peripheral organs (small intestine, kidneys, spleen, and liver)
1003 of mice bearing orthotopic xenografts of U87 cells and treated with either PBS, 200 mg/kg EdU,
1004 5 mg/kg TMZ, or 5 mg/kg TMZ + 200 mg/kg EdU. Abbreviations: 200 mg/kg EdU abbreviated as
1005 "EdU", 5 mg/kg TMZ abbreviated as "TMZ", 5 mg/kg TMZ + 200 mg/kg EdU abbreviated as
1006 "TMZ+EdU". Grading: 0=no finding; 1=minimal finding; 2=mild finding; 3=moderate finding;
1007 4=marked finding; 5=severe finding.

1008 **Figure S6: Mean body weight and mean body weight change of the mice bearing orthotopic**
1009 **xenografts of U87 (A), GBM8 (B), or LN229 (C) cells.**

1010 **Figure S7: Complete blood counts for mice bearing orthotopic xenografts of LN229 cells**
1011 **treated with either PBS, 200 mg/kg EdU, 5 mg/kg TMZ, 5 mg/kg TMZ + 200 mg/kg EdU, 1**
1012 **mg/kg TMZ, or 1 mg/kg TMZ + 200 mg/kg EdU on Days 16, 30 and 58.** Complete counts of
1013 white blood cells (WBCs) **(A)**, lymphocytes (LYMPH) **(B)**, neutrophils **(C)**, basophils (BASO) **(D)**,
1014 eosinophils (EO) **(E)**, and red blood cells (RBC) **(F)** for mice bearing orthotopic xenografts of
1015 LN229 cells treated with either PBS, 200 mg/kg EdU, 5 mg/kg TMZ, 5 mg/kg TMZ + 200 mg/kg
1016 EdU, 1 mg/kg TMZ, or 1 mg/kg TMZ + 200 mg/kg EdU on Days 16, 30 and 58. Lower limit of 95%
1017 CI of mean blood counts for female BALB/c nude mice (n=136): White blood cells: 2.97 K/μL,
1018 lymphocytes: 1.25 K/μL, neutrophils: 1.02 K/μL, basophils: 0.00 K/μL, eosinophils: 0.01 K/μL,
1019 and red blood cells: 8.87 M/μL. One-way ANOVA, *$p<0.05$. Abbreviations: 200 mg/kg EdU
1020 abbreviated as "EdU", 5 mg/kg TMZ abbreviated as "TMZ (H)", 5 mg/kg TMZ + 200 mg/kg EdU
1021 abbreviated as "TMZ (H) + EdU", 1 mg/kg TMZ abbreviated as "TMZ (L)", and 1 mg/kg TMZ +
1022 200 mg/kg EdU abbreviated as "TMZ (L) + EdU".

1023

1024

1025

1026

1027

1028

1029

1030

1031

1032

1033

1034

1035

1036

1037

Figure 1

A

Temozolomide (TMZ)

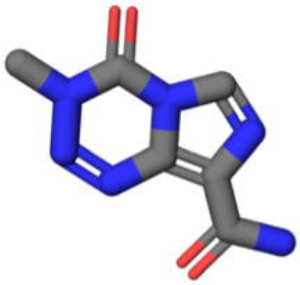

B

5-ethynyl-2'-deoxyuridine (EdU)

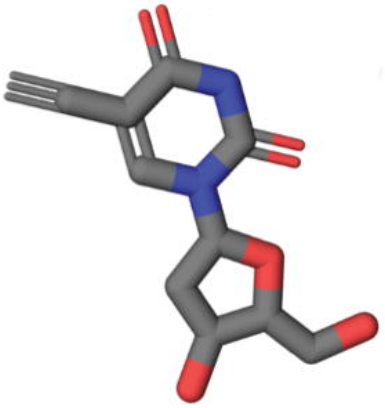

Figure 2

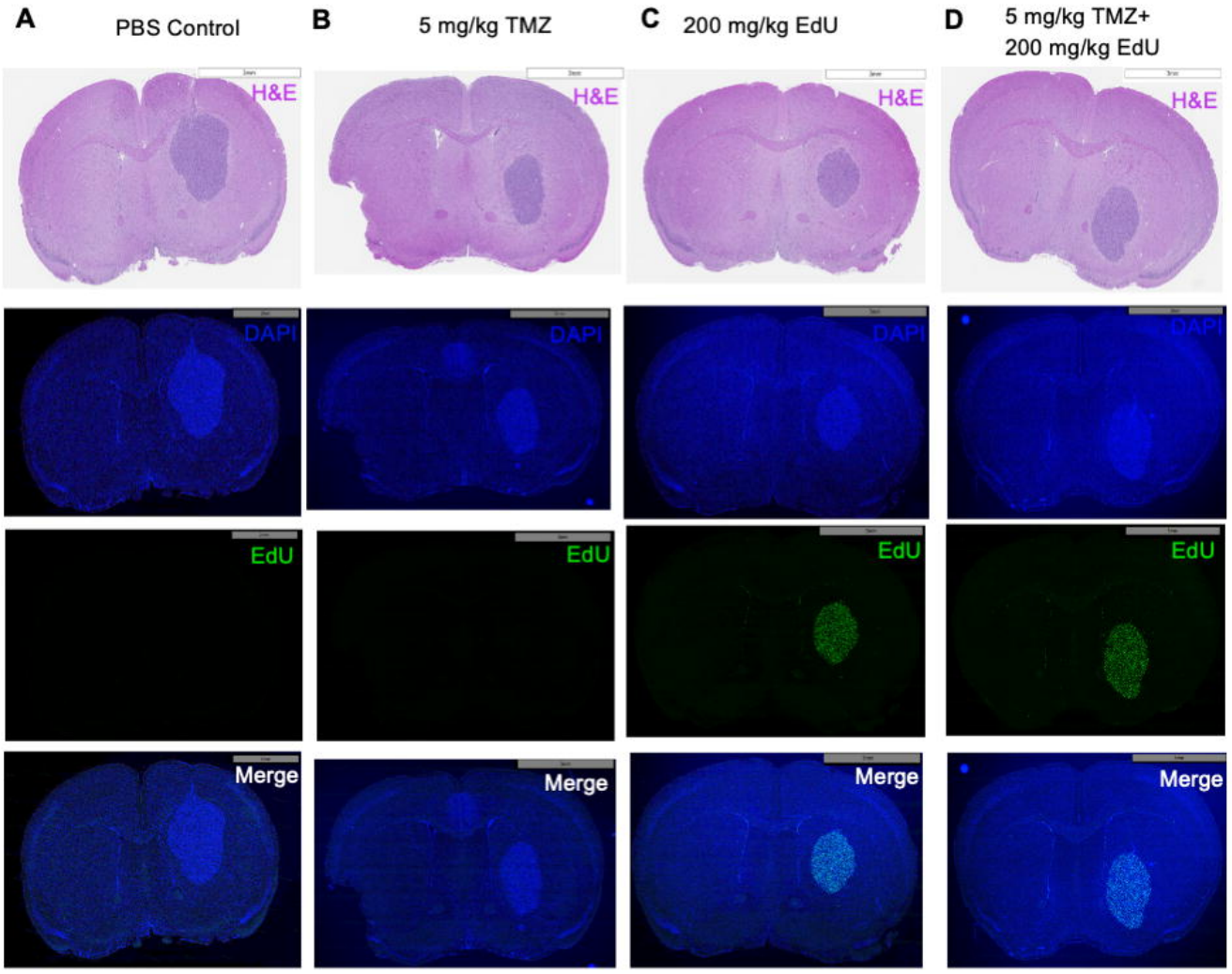
A
PBS Control
B
5 mg/kg TMZ
C
200 mg/kg EdU
D
5 mg/kg TMZ+
200 mg/kg EdU
H&E
DAPI
EdU
Merge

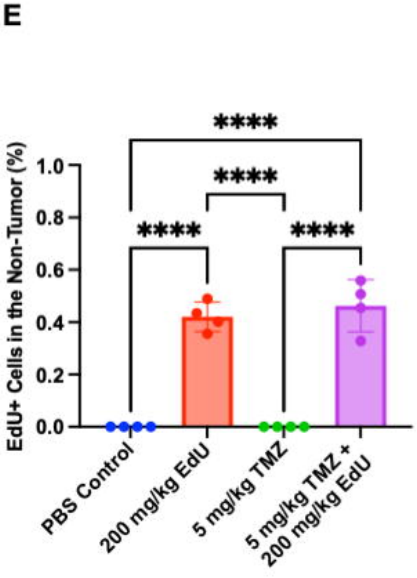
E
EdU+ Cells in the Non-Tumor (%)
1.0
0.8
0.6
0.4
0.2
0.0
****
****
****
PBS Control
200 mg/kg EdU
5 mg/kg TMZ
5 mg/kg TMZ +
200 mg/kg EdU

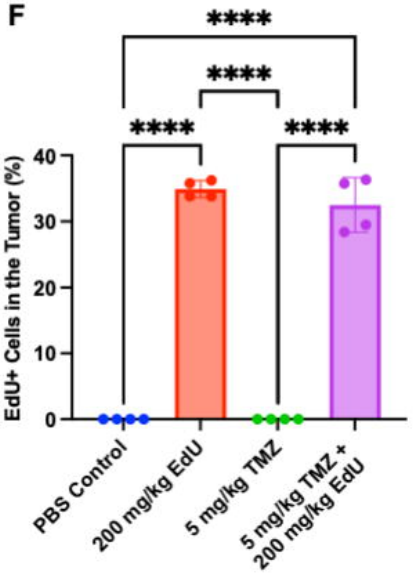
F
EdU+ Cells in the Tumor (%)
40
30
20
10
0
****
****
****
****
PBS Control
200 mg/kg EdU
5 mg/kg TMZ
5 mg/kg TMZ +
200 mg/kg EdU

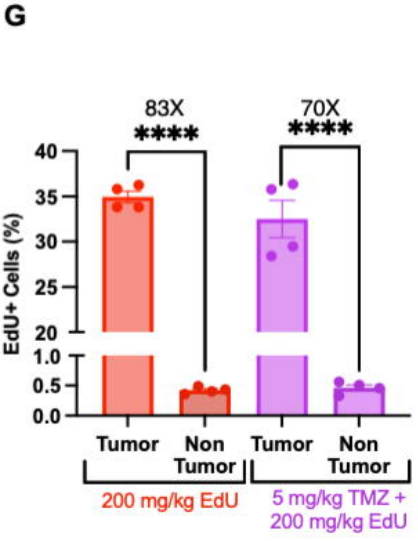
G
83X
70X
****
****
EdU+ Cells (%)
40
35
30
25
20
1.0
0.5
0.0
Tumor
Non
Tumor
Tumor
Non
Tumor
200 mg/kg EdU
5 mg/kg TMZ +
200 mg/kg EdU

Figure 3

A

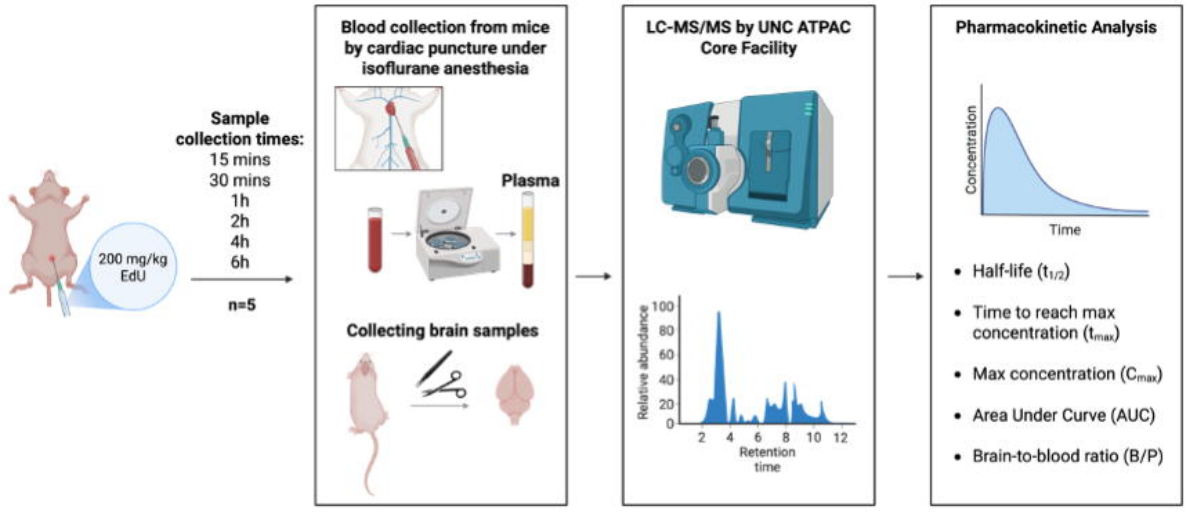

B

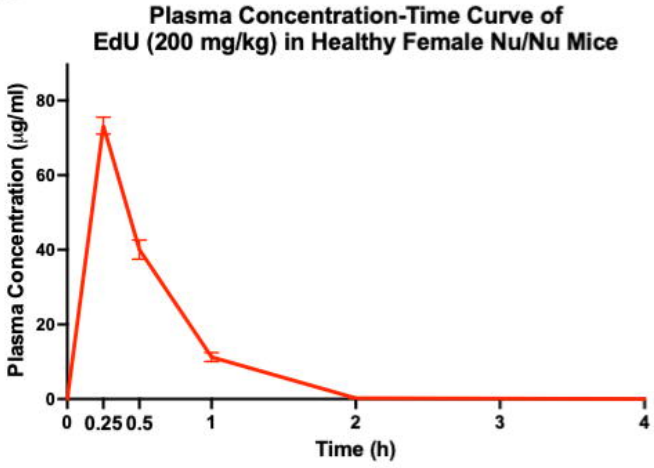

Plasma Pharmacokinetic Parameters of EdU in Healthy Nu/Nu/ Mice	
$AUC_{0\text{-}4h}$ (µ.h/ml)	42.14 ± 2.54
$AUC_{0\text{-}\infty}$ (µ.h/ml)	42.14 ± 2.54
C_{max} (µg/ml)	73.25 ± 2.28
t_{max} (h)	0.25
$t_{1/2}$ (h)	0.19 ± 0.01
CL/F (ml/h)	125.12 ± 7.14
V_d (ml)	34.56 ± 0.3

C

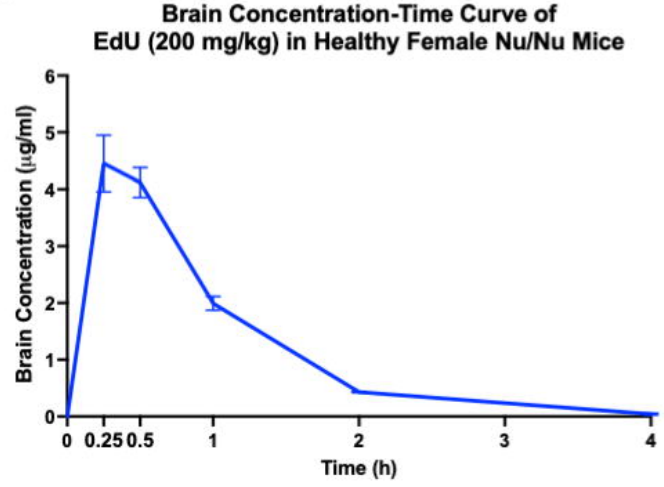

Brain Pharmacokinetic Parameters of EdU in Healthy Nu/Nu/ Mice	
$AUC_{0\text{-}4h}$ (µ.h/ml)	4.89 ± 0.18
$AUC_{0\text{-}\infty}$ (µ.h/ml)	4.92 ± 0.2
C_{max} (µg/ml)	4.78 ± 0.45
t_{max} (h)	0.25
$t_{1/2}$ (h)	0.45 ± 0.07

Figure 4

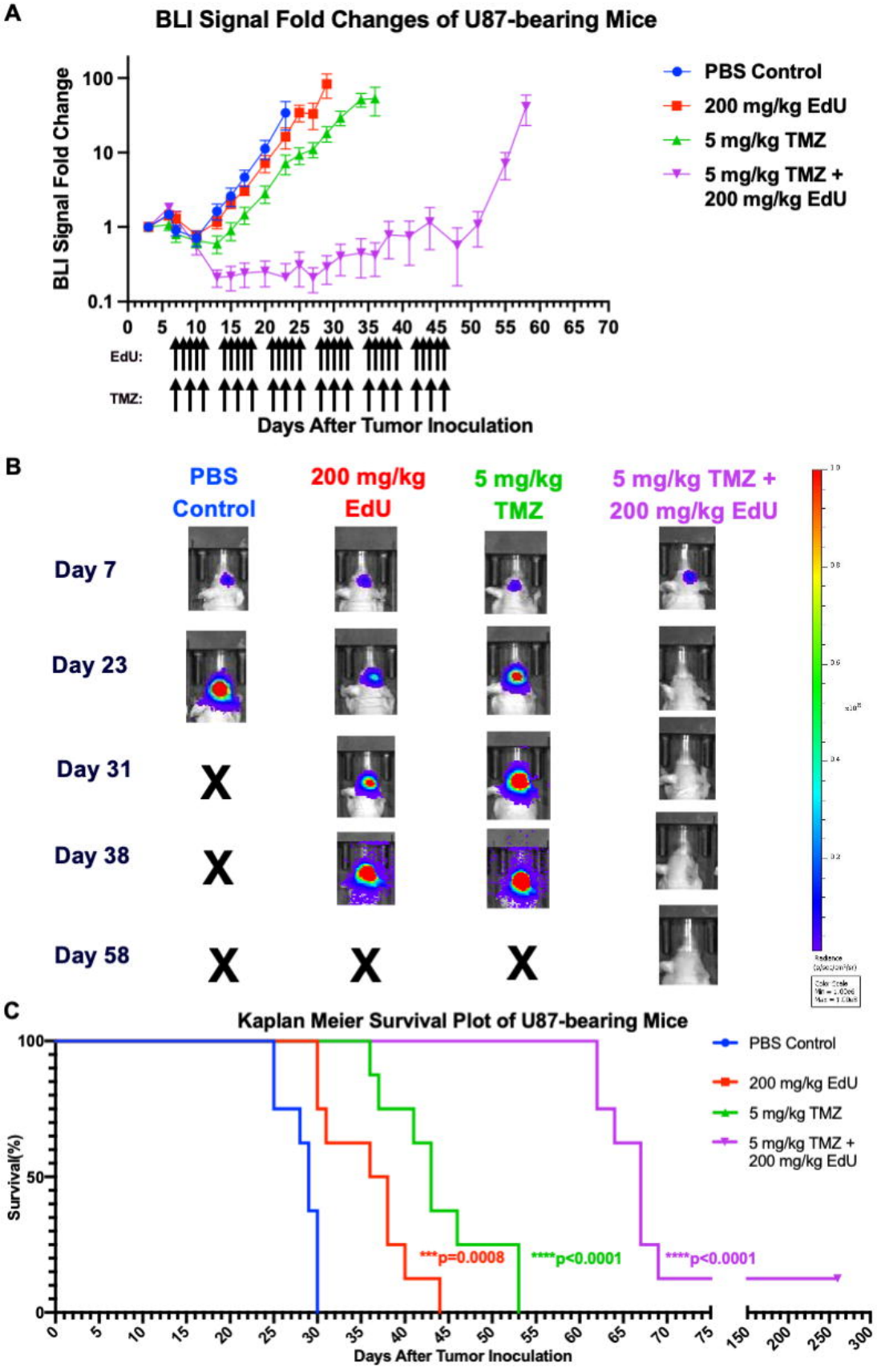
A
BLI Signal Fold Changes of U87-bearing Mice
BLI Signal Fold Change
100
10
1
0.1
0 5 10 15 20 25 30 35 40 45 50 55 60 65 70
EdU:
TMZ:
Days After Tumor Inoculation
PBS Control
200 mg/kg EdU
5 mg/kg TMZ
5 mg/kg TMZ + 200 mg/kg EdU
B
PBS Control
200 mg/kg EdU
5 mg/kg TMZ
5 mg/kg TMZ + 200 mg/kg EdU
Day 7
Day 23
Day 31
Day 38
Day 58
X
C
Kaplan Meier Survival Plot of U87-bearing Mice
Survival(%)
100
50
0
***p=0.0008
****p<0.0001
****p<0.0001
0 5 10 15 20 25 30 35 40 45 50 55 60 65 70 75 150 200 250 300
Days After Tumor Inoculation
PBS Control
200 mg/kg EdU
5 mg/kg TMZ
5 mg/kg TMZ + 200 mg/kg EdU

Figure 5

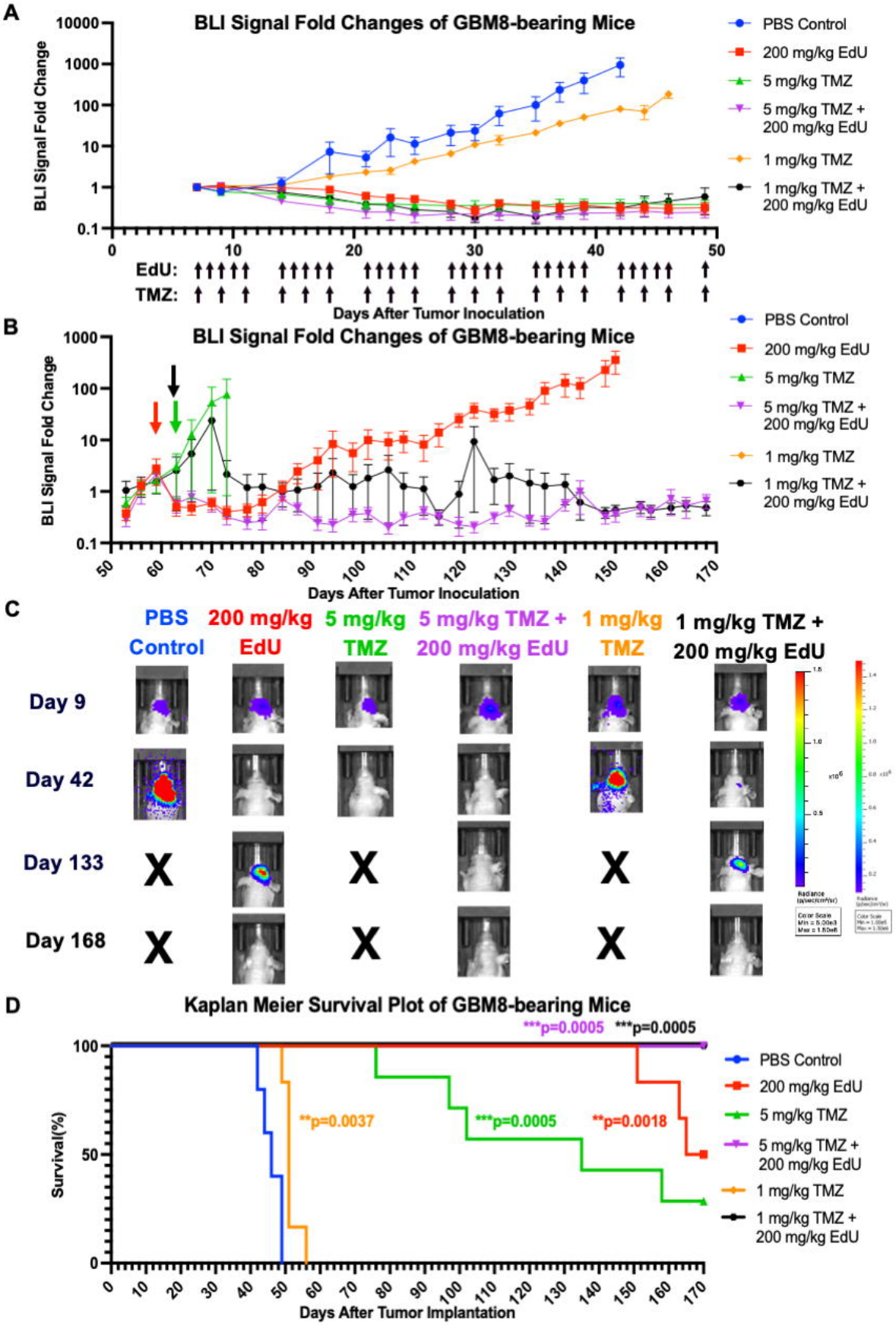
A
BLI Signal Fold Changes of GBM8-bearing Mice
BLI Signal Fold Change
10000
1000
100
10
1
0.1
0
10
20
30
40
50
EdU:
TMZ:
Days After Tumor Inoculation
PBS Control
200 mg/kg EdU
5 mg/kg TMZ
5 mg/kg TMZ + 200 mg/kg EdU
1 mg/kg TMZ
1 mg/kg TMZ + 200 mg/kg EdU
B
BLI Signal Fold Changes of GBM8-bearing Mice
BLI Signal Fold Change
1000
100
10
1
0.1
50
60
70
80
90
100
110
120
130
140
150
160
170
Days After Tumor Inoculation
PBS Control
200 mg/kg EdU
5 mg/kg TMZ
5 mg/kg TMZ + 200 mg/kg EdU
1 mg/kg TMZ
1 mg/kg TMZ + 200 mg/kg EdU
C
PBS Control
200 mg/kg EdU
5 mg/kg TMZ
5 mg/kg TMZ + 200 mg/kg EdU
1 mg/kg TMZ
1 mg/kg TMZ + 200 mg/kg EdU
Day 9
Day 42
Day 133
Day 168
X
D
Kaplan Meier Survival Plot of GBM8-bearing Mice
***p=0.0005
***p=0.0005
**p=0.0037
***p=0.0005
**p=0.0018
Survival(%)
100
50
0
0
10
20
30
40
50
60
70
80
90
100
110
120
130
140
150
160
170
Days After Tumor Implantation
PBS Control
200 mg/kg EdU
5 mg/kg TMZ
5 mg/kg TMZ + 200 mg/kg EdU
1 mg/kg TMZ
1 mg/kg TMZ + 200 mg/kg EdU

Figure 6

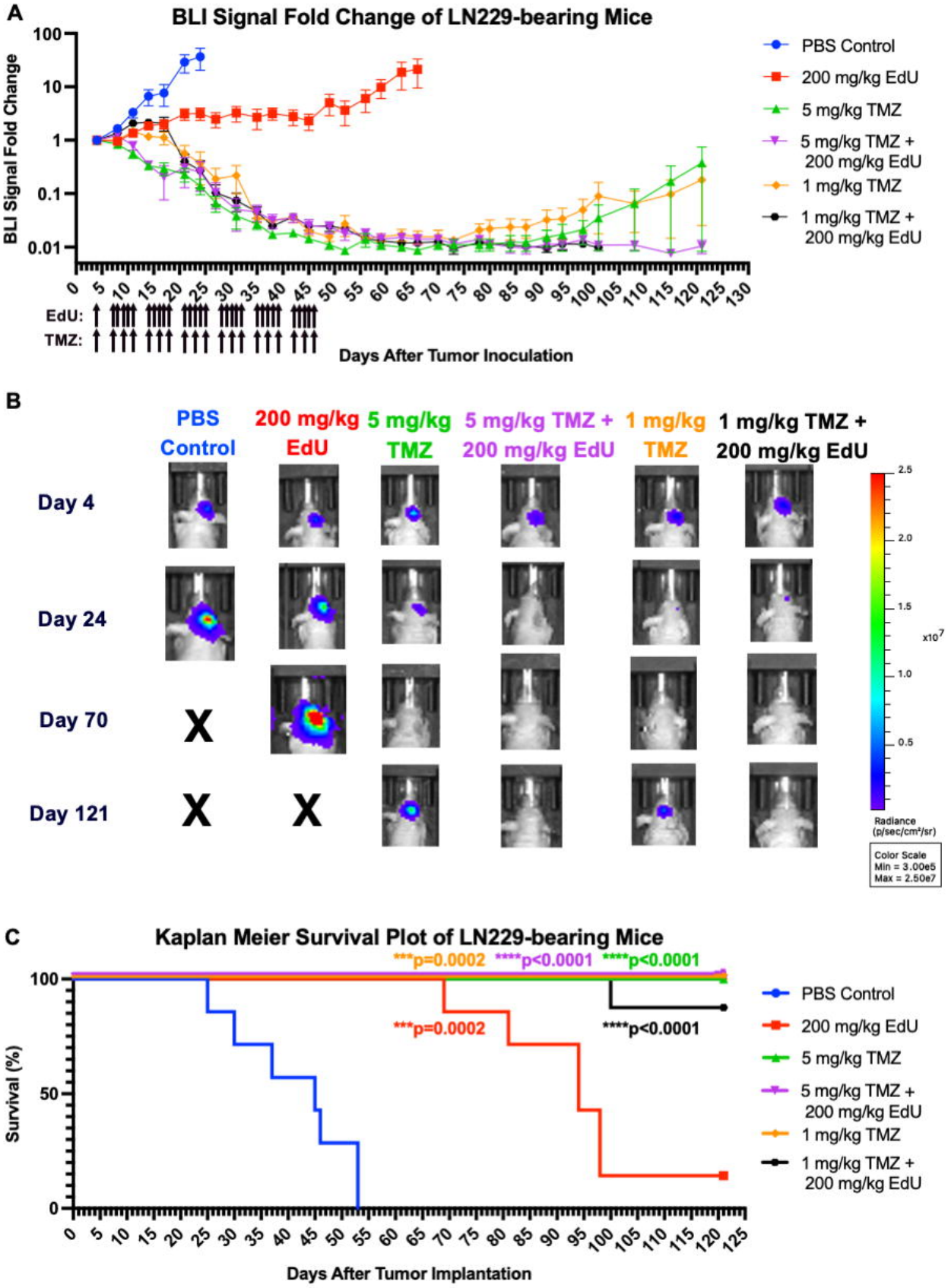
A
BLI Signal Fold Change of LN229-bearing Mice
BLI Signal Fold Change
100
10
1
0.1
0.01
0 5 10 15 20 25 30 35 40 45 50 55 60 65 70 75 80 85 90 95 100 105 110 115 120 125 130
EdU:
TMZ:
Days After Tumor Inoculation
PBS Control
200 mg/kg EdU
5 mg/kg TMZ
5 mg/kg TMZ + 200 mg/kg EdU
1 mg/kg TMZ
1 mg/kg TMZ + 200 mg/kg EdU
B
PBS Control
200 mg/kg EdU
5 mg/kg TMZ
5 mg/kg TMZ + 200 mg/kg EdU
1 mg/kg TMZ
1 mg/kg TMZ + 200 mg/kg EdU
Day 4
Day 24
Day 70
Day 121
X
X
X
2.5
2.0
1.5
x10^7
1.0
0.5
Radiance (p/sec/cm²/sr)
Color Scale
Min = 3.00e5
Max = 2.50e7
C
Kaplan Meier Survival Plot of LN229-bearing Mice
***p=0.0002
****p<0.0001
****p<0.0001
***p=0.0002
****p<0.0001
Survival (%)
100
50
0
0 5 10 15 20 25 30 35 40 45 50 55 60 65 70 75 80 85 90 95 100 105 110 115 120 125
Days After Tumor Implantation
PBS Control
200 mg/kg EdU
5 mg/kg TMZ
5 mg/kg TMZ + 200 mg/kg EdU
1 mg/kg TMZ
1 mg/kg TMZ + 200 mg/kg EdU

Figure 7

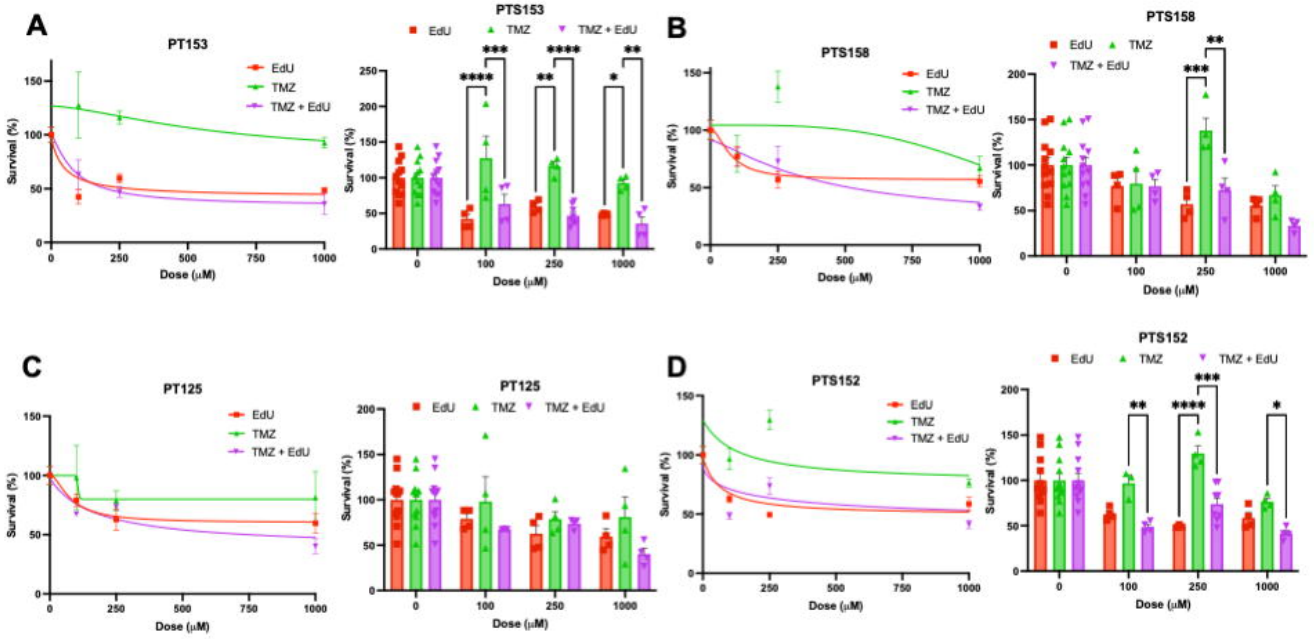

E

Patient ID	Drug1	Drug2	ZIP Synergy Score	ZIP Synergy p value	Status of Interaction Between Drugs
153	EdU	TMZ	14.3	5.06E-02	Synergistic
158	EdU	TMZ	3.0	4.64E-01	Additive
125	EdU	TMZ	2.7	7.07E-01	Additive
152	EdU	TMZ	2.2	7.75E-01	Additive

F

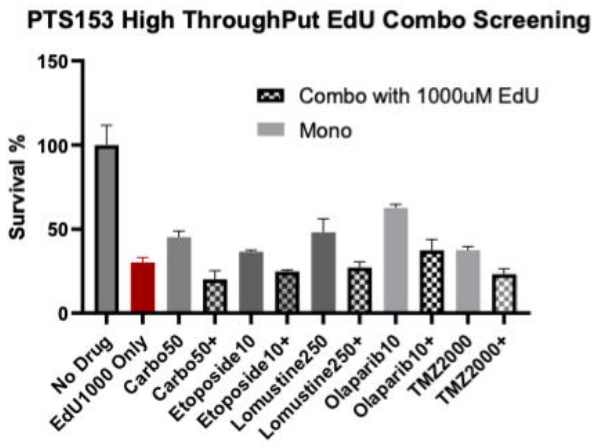
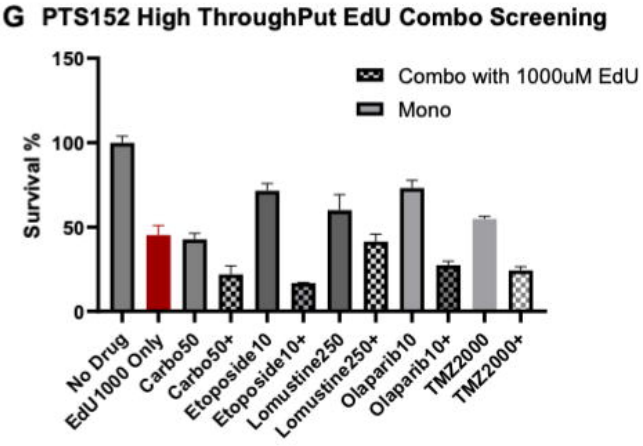
G